INTERNATIONAL JOURNAL OF
NUMERICAL ANALYSIS AND MODELING
Volume 15, Number 4-5, Pages 492–519

AN ENSEMBLE-BASED CONVENTIONAL TURBULENCE MODEL FOR FLUID-FLUID INTERACTION

JEFFREY M. CONNORS

(Communicated by L. Rebholz)

Dedicated to Professor William J. Layton on the occasion of his 60^{th} birthday

Abstract. A statistical turbulence model is proposed for ensemble calculations with two fluids coupled across a flat interface, motivated by atmosphere-ocean interaction. For applications, like climate research, the response of an equilibrium climate state to variations in forcings is important to interrogate predictive capabilities of simulations. The method proposed here focuses on the computation of the ensemble mean-flow fluid velocities. In particular, a closure model is used for the Reynolds stresses that accounts for the fluid behavior at the interface. The model is shown to converge at long times to statistical equilibrium and an analogous, discrete result is shown for two numerical methods. Some matrix assembly costs are reduced with this approach. Computations are performed with monolithic (implicit) and partitioned coupling of the fluid velocities; the former being too expensive for practical computing, but providing a point of comparison to see the effect of partitioning on the ensemble statistics. It is observed that the partitioned methods reproduce the mean-flow behavior well, but may introduce some long-time statistical bias.

Key words. Atmosphere-ocean, variance, statistical equilibrium

1. Introduction

Ensemble calculations with global circulation models (GCMs) are an important component of climate variability studies. Many long-time integrations are performed to assess the average near-surface temperature change in response to changes in forcings for the climate system at radiative equilibrium. There are multiple sources of uncertainty in calculated responses. For a given computational model, some studies focus on parametric uncertainty (see [8], 9.2.2.2). One way to mitigate cost is to apply statistical models for simulation responses that require only a modest number of uncertain parameters and ensemble members, for example in perturbed physics ensemble methods (*e.g.* [22]). Given a moderate number of ensembles, this paper investigates another possible cost-reduction measure. Based on the work of Jiang, Kaya and Layton [10], a method is proposed herein to compute ensemble-mean flow states efficiently, by using a conventional (statistical) turbulence model (CTM). CTM models (like RANS [1] or $k-\epsilon$ [20]) seek to reduce the number of degrees of freedom required to resolve mean fluid behavior. The method has the additional benefit of reducing some matrix-assembly costs for the ensemble computations.

The focus is on atmosphere-ocean interaction (AOI). A key aspect of many AOI models is to avoid resolving the boundary layers, instead relying on boundary conditions that conserve fluxes across the layers. In order to reduce the problem down but retain this key mathematical detail, Connors, Howell and Layton investigated a model of two incompressible fluids coupled across a flat interface [5]. A similar model is adopted here, since it provides a convenient setting in which to incorporate

Received by the editors December 30, 2016, and in revised form, April 28, 2017.
1991 *Mathematics Subject Classification.* 76F55,65Z05,65M60.

the work of Jiang, Kaya and Layton. However, it is necessary to account for the special dynamics in AOI introduced by the differences in vertical versus horizontal scaling, and also by the interface boundary conditions.

1.1. A conventional turbulence model for coupled fluids. Consider an ensemble of velocities and pressures for flows in the atmosphere and ocean (domains $\Omega_{\mathcal{A}}, \Omega_{\mathcal{O}} \subset \mathbb{R}^d$, $d = 2, 3$, respectively), satisfying

$$\partial_t \mathbf{u}_j - \mathcal{D}_{\mathcal{A}}(\mathbf{u}_j) + \mathbf{u}_j \cdot \nabla \mathbf{u}_j + \nabla p_j = \mathbf{f}_{\mathcal{A}j} \text{ on } \Omega_{\mathcal{A}} \times (0,T], \tag{1}$$

$$\nabla \cdot \mathbf{u}_j = 0 \text{ on } \Omega_{\mathcal{A}} \times (0,T], \tag{2}$$

$$\mathbf{u}_j(\mathbf{x}, t=0) = \mathbf{u}_j^0(\mathbf{x}) \text{ on } \Omega_{\mathcal{A}}, \tag{3}$$

$$\partial_t \mathbf{v}_j - \mathcal{D}_{\mathcal{O}}(\mathbf{v}_j) + \mathbf{v}_j \cdot \nabla \mathbf{v}_j + \nabla q_j = \mathbf{f}_{\mathcal{O}j} \text{ on } \Omega_{\mathcal{O}} \times (0,T], \tag{4}$$

$$\nabla \cdot \mathbf{v}_j = 0 \text{ on } \Omega_{\mathcal{O}} \times (0,T], \tag{5}$$

$$\mathbf{v}_j(\mathbf{x}, t=0) = \mathbf{v}_j^0(\mathbf{x}) \text{ on } \Omega_{\mathcal{O}}. \tag{6}$$

Here, $\mathcal{D}_{\mathcal{A}}(\mathbf{u}_j)$ and $\mathcal{D}_{\mathcal{O}}(\mathbf{v}_j)$ are viscosity terms. Let $\mathbf{D}(\mathbf{u})$ represent any $d \times d$ tensor or matrix, with entries $\mathbf{D}(\mathbf{u})_{ij}$, $1 \le i, j \le d$. Define a decomposition by

$$\begin{aligned} \mathbf{D}(\mathbf{u}) &= \mathbf{D}(\mathbf{u})^H + \mathbf{D}(\mathbf{u})^\perp, \\ \left(\mathbf{D}(\mathbf{u})^H\right)_{ij} &= \begin{cases} (\mathbf{D}(\mathbf{u}))_{ij} & \text{for } i = 1, \dots, d-1,\ j = 1, \dots, d, \\ 0, & \text{otherwise} \end{cases} \\ \left(\mathbf{D}(\mathbf{u})^\perp\right)_{ij} &= \begin{cases} (\mathbf{D}(\mathbf{u}))_{ij} & \text{for } i = d,\ j = 1, \dots, d, \\ 0, & \text{otherwise} \end{cases} \end{aligned} \tag{7}$$

Now let $\mathbf{D}(\mathbf{u}) = (\nabla \mathbf{u} + \nabla \mathbf{u}^T)/2$ be specifically the viscous part of the Cauchy stress tensor. The diffusion terms are decomposed into horizontal and vertical terms:

$$\mathcal{D}_{\mathcal{A}}(\mathbf{u}_j) = 2\nabla \cdot \left({\nu_{\mathcal{A}}}^H \mathbf{D}(\mathbf{u}_j)^H + {\nu_{\mathcal{A}}}^\perp \mathbf{D}(\mathbf{u}_j)^\perp \right), \tag{8}$$

$$\mathcal{D}_{\mathcal{O}}(\mathbf{v}_j) = 2\nabla \cdot \left({\nu_{\mathcal{O}}}^H \mathbf{D}(\mathbf{v}_j)^H + {\nu_{\mathcal{O}}}^\perp \mathbf{D}(\mathbf{v}_j)^\perp \right). \tag{9}$$

The constants ${\nu_{\mathcal{A}}}^H > 0$ and ${\nu_{\mathcal{O}}}^H > 0$ are horizontal diffusion parameters, whereas ${\nu_{\mathcal{A}}}^\perp > 0$ and ${\nu_{\mathcal{O}}}^\perp > 0$ are (constant) vertical diffusion parameters. The horizontal scale is much larger than the vertical scale for atmosphere-ocean simulations. Due to the nature of flow features that result from this scale discrepancy, it is typical in practice to treat horizontal and vertical diffusion processes differently (see, *e.g.* [21, 23]). While many other aspects of typical atmosphere-ocean models are not included here, the above model retains the necessary mathematical features for the investigation in this paper. Boundary conditions are discussed later.

We assume that $j = 1, \dots, J$ and define the ensemble average, say a, of any collection of J objects a_j by

$$a \equiv < a_j > \equiv \frac{1}{J} \sum_{j=1}^{J} a_j. \tag{10}$$

A model for the ensemble-averaged mean flow is

$$\partial_t \mathbf{u} - \mathcal{D}_{\mathcal{A}}(\mathbf{u}) + \mathbf{u} \cdot \nabla \mathbf{u} + \nabla p - \nabla \cdot R(\mathbf{u}, \mathbf{u}) = \mathbf{f}_{\mathcal{A}} \text{ on } \Omega_{\mathcal{A}} \times (0,T], \tag{11}$$

$$\nabla \cdot \mathbf{u} = 0 \text{ on } \Omega_{\mathcal{A}} \times (0,T], \tag{12}$$

$$\mathbf{u}(\mathbf{x}, t=0) = \mathbf{u}_0(\mathbf{x}) \text{ on } \Omega_{\mathcal{A}}, \tag{13}$$

$$\partial_t \mathbf{v} - \mathcal{D}_{\mathcal{O}}(\mathbf{v}) + \mathbf{v} \cdot \nabla \mathbf{v} + \nabla q - \nabla \cdot R(\mathbf{v}, \mathbf{v}) = \mathbf{f}_{\mathcal{O}} \text{ on } \Omega_{\mathcal{O}} \times (0,T], \tag{14}$$

$$\nabla \cdot \mathbf{v} = 0 \text{ on } \Omega_{\mathcal{O}} \times (0,T], \tag{15}$$

$$\mathbf{v}(\mathbf{x}, t=0) = \mathbf{v}_0(\mathbf{x}) \text{ on } \Omega_{\mathcal{O}}, \tag{16}$$

where the (yet to be closed) Reynolds stresses are denoted by

$$R(\mathbf{u},\mathbf{u}) \equiv < \mathbf{u}_j >< \mathbf{u}_j > - < \mathbf{u}_j\mathbf{u}_j > .$$

The key is what happens at the interface between the fluids, which are coupled across a flat interface, Γ_I. The coupling is based on the so-called "rigid-lid" hypothesis that has often been used for atmosphere-ocean coupling; that small-scale fluctuations can be eliminated by using a flat ocean surface model and still capture the correct long-time statistical behavior. Also, the boundary layers of the atmosphere and ocean are not resolved but are instead replaced by using formulae for the bulk transfer of physical fluxes between the fluids. A full description of the primitive equations of the coupled atmosphere-ocean system and their mathematical analysis is found in the papers of Lions, Temam and Wang [16, 17, 18].

Let the outward-pointing normal vectors of unit length on the boundaries of $\Omega_{\mathcal{A}}$ and $\Omega_{\mathcal{O}}$ be denoted by $\hat{\mathbf{n}}_{\mathcal{A}}$ and $\hat{\mathbf{n}}_{\mathcal{O}}$, respectively. A generic unit vector $\hat{\boldsymbol{\tau}}$ is also used, defined by $\hat{\boldsymbol{\tau}} = (\pm 1, 0)$ $(d = 2)$ or $\hat{\boldsymbol{\tau}} = (\tau_1, \tau_2, 0)$ $(d = 3)$. On the interface the fluids cannot penetrate and the transfer of horizontal momentum across the boundary layers is represented using a slip-with-friction condition:

$$\begin{gathered} \mathbf{u}_j \cdot \hat{\mathbf{n}}_{\mathcal{A}} = \mathbf{v}_j \cdot \hat{\mathbf{n}}_{\mathcal{O}} = 0, \\ -\rho_{\mathcal{A}}{\nu_{\mathcal{A}}}^{\perp}\hat{\mathbf{n}}_{\mathcal{A}} \cdot \nabla \mathbf{u}_j \cdot \hat{\boldsymbol{\tau}} = \rho_{\mathcal{O}}{\nu_{\mathcal{O}}}^{\perp}\hat{\mathbf{n}}_{\mathcal{O}} \cdot \nabla \mathbf{v}_j \cdot \hat{\boldsymbol{\tau}} = \rho_{\mathcal{A}}\kappa_j \left|\mathbf{u}_j - \mathbf{v}_j\right| (\mathbf{u}_j - \mathbf{v}_j) \cdot \hat{\boldsymbol{\tau}} \end{gathered} \tag{17}$$

on $\Gamma_I \times (0, T]$. The parameters $\rho_{\mathcal{A}} > 0$ and $\rho_{\mathcal{O}} > 0$ are densities. The friction parameters $\kappa_j > 0$ are calculated in practice from bulk flux formulae that involve other variables not considered in the above model, but which may be viewed as introducing additional sources of uncertainty. These parameters will be time dependent, but for simplicity their dependence on $\mathbf{x}$ is neglected in this paper. Furthermore, these values should remain bounded away from zero and infinity. It is assumed herein that $\kappa_j(t) \in \mathcal{C}^{\infty}(0, \infty)$ and

$$0 < \kappa_0 \leq \kappa_j(t) < \kappa_{\infty} < \infty, \quad j = 1, \ldots, J, \tag{18}$$

for all $t \in [0, \infty)$, where κ_0 and κ_{∞} are independent of time and j.

Upon ensemble averaging of (17), we see

$$\begin{gathered} \mathbf{u} \cdot \hat{\mathbf{n}}_{\mathcal{A}} = \mathbf{v} \cdot \hat{\mathbf{n}}_{\mathcal{O}} = 0, \\ -\rho_{\mathcal{A}}{\nu_{\mathcal{A}}}^{\perp}\hat{\mathbf{n}}_{\mathcal{A}} \cdot \nabla \mathbf{u} \cdot \hat{\boldsymbol{\tau}} = \rho_{\mathcal{O}}{\nu_{\mathcal{O}}}^{\perp}\hat{\mathbf{n}}_{\mathcal{O}} \cdot \nabla \mathbf{v} \cdot \hat{\boldsymbol{\tau}} = \rho_{\mathcal{A}} \left\langle \kappa_j \left|\mathbf{u}_j - \mathbf{v}_j\right| (\mathbf{u}_j - \mathbf{v}_j) \right\rangle \cdot \hat{\boldsymbol{\tau}}, \end{gathered} \tag{19}$$

which adds another consideration for the closure problem, since (for example)

$$\left\langle \kappa_j \left|\mathbf{u}_j - \mathbf{v}_j\right| (\mathbf{u}_j - \mathbf{v}_j) \right\rangle \cdot \hat{\boldsymbol{\tau}} \neq \kappa \left|\mathbf{u} - \mathbf{v}\right| (\mathbf{u} - \mathbf{v}) \cdot \hat{\boldsymbol{\tau}}.$$

The focus of this paper is the computation of ensembles for the coupled fluid-fluid model, for which purpose it shall not be necessary to derive a theoretical boundary condtion for the mean-flow transfer of momentum across the interface. It shall be shown that only individual realizations $(\mathbf{u}_j, \mathbf{v}_j)$ will need to be computed, for which purpose it suffices to apply the correct boundary conditions (17). Then the identities (19) will hold automatically at each discrete time level. The closure problem associated with the mean-flow transfer of momentum across the interface is left as an interesting open problem for purposes of theoretical analysis.

TABLE 1. Choices for turbulent mixing lengths and turbulent energies.

	$\widetilde{\nu_{\mathcal{A}}}^H$	$\widetilde{\nu_{\mathcal{A}}}^\perp$	$\widetilde{\nu_{\mathcal{O}}}^H$	$\widetilde{\nu_{\mathcal{O}}}^\perp$
l	$\Delta t < \lvert(\mathbf{u}_j^H)'\rvert >$	$\Delta t < \lvert(\mathbf{u}_j^\perp)'\rvert >$	$\Delta t < \lvert(\mathbf{v}_j^H)'\rvert >$	$\Delta t < \lvert(\mathbf{v}_j^\perp)'\rvert >$
k'	$\frac{\rho_{\mathcal{A}}}{2} < \lvert(\mathbf{u}_j^H)'\rvert^2 >$	$\frac{\rho_{\mathcal{A}}}{2} < \lvert(\mathbf{u}_j^\perp)'\rvert^2 >$	$\frac{\rho_{\mathcal{O}}}{2} < \lvert(\mathbf{v}_j^H)'\rvert^2 >$	$\frac{\rho_{\mathcal{O}}}{2} < \lvert(\mathbf{v}_j^\perp)'\rvert^2 >$

The critical issue is to model the behavior of the Reynolds stresses. Apply the eddy viscosity (EV) hypothesis away from boundaries and approximate

$$\begin{aligned} \nabla \cdot R(\mathbf{u},\mathbf{u}) &\approx \mathcal{D}_{\mathcal{A}}{}^T(\mathbf{u}) + \text{ model pressure terms, in } \Omega_{\mathcal{A}} \\ \mathcal{D}_{\mathcal{A}}{}^T(\mathbf{u}) &\equiv 2\nabla\cdot\left(\widetilde{\nu_{\mathcal{A}}}^H\mathbf{D}(\mathbf{u})^H + \widetilde{\nu_{\mathcal{A}}}^\perp\mathbf{D}(\mathbf{u})^\perp\right) \end{aligned} \tag{20}$$

$$\begin{aligned} \text{and } \nabla \cdot R(\mathbf{v},\mathbf{v}) &\approx \mathcal{D}_{\mathcal{O}}{}^T(\mathbf{v}) + \text{ model pressure terms, in } \Omega_{\mathcal{O}}, \\ \mathcal{D}_{\mathcal{O}}{}^T(\mathbf{v}) &\equiv 2\nabla\cdot\left(\widetilde{\nu_{\mathcal{O}}}^H\mathbf{D}(\mathbf{v})^H + \widetilde{\nu_{\mathcal{O}}}^\perp\mathbf{D}(\mathbf{v})^\perp\right). \end{aligned} \tag{21}$$

Here, $\widetilde{\nu_{\mathcal{A}}}^H, \widetilde{\nu_{\mathcal{O}}}^H, \widetilde{\nu_{\mathcal{A}}}^\perp, \widetilde{\nu_{\mathcal{O}}}^\perp$ are turbulent viscosities in the bulk atmosphere and ocean. Their dependence on turbulent fluctuations shall be prescribed via the Kolmogorov-Prandtl relationship

$$\nu^T = \sqrt{2}\mu l\sqrt{k'}, \tag{22}$$

where ν^T denotes a turbulent viscosity parameter, μ is a tuning parameter, l is a subscale mixing length and k' is the kinetic energy associated with turbulent fluctuations.

The key is to choose l and k' such that these values will naturally vanish near boundaries, but away from boundaries they yield reasonable results to model subscale diffusion. First, define fluctuations a_j' for data $a_1, \ldots, a_J$ by

$$a_j' \equiv a_j - < a_j >,\ j = 1, \ldots, J.$$

Velocities will be decomposed into horizontal and vertical components:

$$\mathbf{u}_j = \mathbf{u}_j^H + \mathbf{u}_j^\perp, \quad \mathbf{v}_j = \mathbf{v}_j^H + \mathbf{v}_j^\perp,$$

where $\mathbf{u}_j^H, \mathbf{v}_j^H$ are the horizontal components and $\mathbf{u}_j^\perp, \mathbf{v}_j^\perp$ are the vertical components. Then the turbulent viscosities are specified by choosing l and k' as shown in Table 1. The choices for l represent the (average) distance a turbulent, subscale feature moves (either horizontally or vertically) in a time Δt, shown in [9] to yield good results. The values for k' represent the (average) kinetic energy density of a subscale eddy.

Note that on boundaries where a no-slip condition is imposed, these choices of turbulent viscosities will automatically vanish. If a no-penetration condition is imposed, such as at the atmosphere-ocean interface with rigid lid, the vertical component of velocity still vanishes and thus drives the values of $\widetilde{\nu_{\mathcal{A}}}^\perp$ and $\widetilde{\nu_{\mathcal{O}}}^\perp$ to zero. As a result, from (20)-(21) it follows that

$$\begin{aligned} \hat{\mathbf{n}}_{\mathcal{A}} \cdot R(\mathbf{u},\mathbf{u}) \approx 2\widetilde{\nu_{\mathcal{A}}}^\perp \hat{\mathbf{n}}_{\mathcal{A}} \cdot \mathbf{D}(\mathbf{u})^\perp = 0 \\ \text{and } \hat{\mathbf{n}}_{\mathcal{O}} \cdot R(\mathbf{v},\mathbf{v}) \approx 2\widetilde{\nu_{\mathcal{O}}}^\perp \hat{\mathbf{n}}_{\mathcal{O}} \cdot \mathbf{D}(\mathbf{v})^\perp = 0 \end{aligned}$$

on Γ_I. This is consistent with the behavior of the Reynolds stresses at the interface:

$$\begin{aligned} \hat{\mathbf{n}}_{\mathcal{A}} \cdot R(\mathbf{u},\mathbf{u}) &= < \hat{\mathbf{n}}_{\mathcal{A}} \cdot \mathbf{u}_j >< \mathbf{u}_j > - < (\hat{\mathbf{n}}_{\mathcal{A}} \cdot \mathbf{u}_j)\, \mathbf{u}_j >= 0 \\ \text{and } \hat{\mathbf{n}}_{\mathcal{O}} \cdot R(\mathbf{v},\mathbf{v}) &= < \hat{\mathbf{n}}_{\mathcal{O}} \cdot \mathbf{v}_j >< \mathbf{v}_j > - < (\hat{\mathbf{n}}_{\mathcal{O}} \cdot \mathbf{v}_j)\, \mathbf{v}_j >= 0 \ \text{ on } \Gamma_I. \end{aligned}$$

2. Mathematical preliminaries

Coordinates in space are denoted by $\mathbf{x} = (x_1, \ldots, x_d)$. The domains are rectangles ($d = 2$) or boxes ($d = 3$) of the form

$$\begin{aligned} &\Omega_{\mathcal{A}} = (0, L_1) \times (0, H_{\mathcal{A}}) \ \text{ and } \ \Omega_{\mathcal{O}} = (0, L_1) \times (-H_{\mathcal{O}}, 0) \ \ (d = 2) \\ &\Omega_{\mathcal{A}} = (0, L_1) \times (0, L_2) \times (0, H_{\mathcal{A}}) \\ &\text{and } \ \Omega_{\mathcal{O}} = (0, L_1) \times (0, L_2) \times (-H_{\mathcal{O}}, 0) \ \ (d = 3). \end{aligned} \tag{23}$$

The values $H_{\mathcal{A}} > 0$ and $H_{\mathcal{O}} > 0$ represent the height of $\Omega_{\mathcal{A}}$ and the depth of $\Omega_{\mathcal{O}}$. The domain width in the lateral directions are $0 < L_1, L_2$. The domains are coupled across their shared interface $\Gamma_I = \overline{\Omega_{\mathcal{A}}} \cap \overline{\Omega_{\mathcal{O}}}$, which lies in the plane $x_d = 0$. Other boundaries are

$$\begin{aligned} \Gamma_t &= \partial\Omega_{\mathcal{A}} \cap \{x_d = H_{\mathcal{A}}\} \quad \text{(top of atmosphere)} \\ \Gamma_b &= \partial\Omega_{\mathcal{O}} \cap \{x_d = -H_{\mathcal{O}}\} \quad \text{(bottom of ocean)} \\ \Gamma_L^{\mathcal{A}} &= \partial\Omega_{\mathcal{A}} \setminus (\Gamma_t \cup \Gamma_I) \quad \text{(lateral atmosphere boundaries)} \\ \Gamma_L^{\mathcal{O}} &= \partial\Omega_{\mathcal{O}} \setminus (\Gamma_b \cup \Gamma_I) \quad \text{(lateral ocean boundaries)}. \end{aligned} \tag{24}$$

The velocities and pressures are denoted by

$$\begin{aligned} \mathbf{u}_j &= (u_{1,j}, \ldots, u_{d,j}) : \Omega_{\mathcal{A}} \to \mathbb{R}^d, \quad p_j : \Omega_{\mathcal{A}} \to \mathbb{R}, \\ \mathbf{v}_j &= (v_{1,j}, \ldots, v_{d,j}) : \Omega_{\mathcal{O}} \to \mathbb{R}^d, \quad q_j : \Omega_{\mathcal{O}} \to \mathbb{R}. \end{aligned} \tag{25}$$

Periodic lateral boundary conditions are chosen. At the atmosphere top and ocean bottom, a no-slip condition is imposed for the velocities:

$$\mathbf{u}_j = 0 \text{ on } \Gamma_t \times (0, T] \text{ and } \mathbf{v}_j = 0 \text{ on } \Gamma_b \times (0, T]. \tag{26}$$

The ensemble-mean flows then have the same lateral, top and bottom boundary conditions.

Remark 1. *At the atmosphere top, the usual boundary conditions would be no-penetration and no-tangential-stress (also called "no-flux"). However, the no-slip condition is used herein to simplify the analysis and presentation.*

Some preliminary notation and results will be used for purposes of analysis.

Definition 1. Standard L^2-inner-products are defined on each domain by

$$(\mathbf{u}, \widetilde{\mathbf{u}})_{\mathcal{A}} \equiv \int_{\Omega_{\mathcal{A}}} \mathbf{u} \cdot \widetilde{\mathbf{u}} \, d\mathbf{x} \qquad \text{and} \qquad (\mathbf{v}, \widetilde{\mathbf{v}})_{\mathcal{O}} \equiv \int_{\Omega_{\mathcal{O}}} \mathbf{v} \cdot \widetilde{\mathbf{v}} \, d\mathbf{x}.$$

Definition 2.

$$\begin{aligned} \|\mathbf{u}\|_{p,2} &\equiv \left(\int_0^T \|\mathbf{u}\|^p \right)^{1/p}, \ 1 \le p < \infty, \\ \|\mathbf{u}\|_{\infty,2} &\equiv \text{ess sup}_{0 \le t \le T} \|\mathbf{u}(t)\|. \end{aligned}$$

Definition 3. Weak spaces for the velocities and pressures are defined with respect to the above boundary condtions.

$$X_{\mathcal{A}} \equiv \mathrm{cl}_{(H^1)^d}\left\{\mathbf{u} \in \left(\mathcal{C}^\infty(\overline{\Omega_{\mathcal{A}}})\right)^d \,|\, \mathbf{u}(x_i) = \mathbf{u}(x_i + L_i),\ 1 \le i < d,\ \mathbf{u} = 0 \text{ on } \Gamma_t \cup \Gamma_I\right\}.$$

$$X_{\mathcal{O}} \equiv \mathrm{cl}_{(H^1)^d}\left\{\mathbf{v} \in \left(\mathcal{C}^\infty(\overline{\Omega_{\mathcal{O}}})\right)^d \,|\, \mathbf{v}(x_i) = \mathbf{v}(x_i + L_i),\ 1 \le i < d,\ \mathbf{v} = 0 \text{ on } \Gamma_b, v_d = 0 \text{ on } \Gamma_I\right\}.$$

$$P_{\mathcal{A}} \equiv \mathrm{cl}_{H^1}\left\{p \in \mathcal{C}^\infty(\overline{\Omega_{\mathcal{A}}}) \,|\, \int_{\Omega_{\mathcal{A}}} p\, d\mathbf{x} = 0,\ p(x_i) = p(x_i + L_i),\ 1 \le i < d\right\}.$$

$$P_{\mathcal{O}} \equiv \mathrm{cl}_{H^1}\left\{q \in \mathcal{C}^\infty(\overline{\Omega_{\mathcal{O}}}) \,|\, \int_{\Omega_{\mathcal{O}}} q\, d\mathbf{x} = 0,\ q(x_i) = q(x_i + L_i),\ 1 \le i < d\right\}.$$

Divergence-free subspaces are needed for the velocities.

Definition 4.

$$V_{\mathcal{A}} \equiv \{\mathbf{u} \in X_{\mathcal{A}} \,|\, (\nabla \cdot \mathbf{u}, p)_{\mathcal{A}} = 0,\ \forall p \in P_{\mathcal{A}}\} \tag{27}$$

$$V_{\mathcal{O}} \equiv \{\mathbf{v} \in X_{\mathcal{O}} \,|\, (\nabla \cdot \mathbf{v}, q)_{\mathcal{O}} = 0,\ \forall q \in P_{\mathcal{O}}\} \tag{28}$$

Due to the boundary conditions on Γ_I, it is necessary to work with the space $L^3(\Gamma_I)$. It is well-known that traces of functions in $X_{\mathcal{A}}$ and $X_{\mathcal{O}}$ are well-defined in this sense (see *e.g.* [6]). The next definition provides a compact notation.

Definition 5.

$$\|\mathbf{u}\|_I \equiv \left(\int_{\Gamma_I} |\mathbf{u}|^3\, d\Gamma_I\right)^{1/3}.$$

Definition 6. Given functions $\mathbf{u}, \tilde{\mathbf{u}} \in (H^1(\Omega_{\mathcal{A}}))^d$ and $\mathbf{v}, \tilde{\mathbf{v}} \in (H^1(\Omega_{\mathcal{O}}))^d$, some bilinear forms are defined as follows.

$$a_{\mathcal{A}}(\mathbf{u}, \tilde{\mathbf{u}}) \equiv 2{\nu_{\mathcal{A}}}^H \int_{\Omega_{\mathcal{A}}} \mathbf{D}(\mathbf{u})^H : \nabla\tilde{\mathbf{u}}\, d\mathbf{x} + 2{\nu_{\mathcal{A}}}^\perp \int_{\Omega_{\mathcal{A}}} \mathbf{D}(\mathbf{u})^\perp : \nabla\tilde{\mathbf{u}}\, d\mathbf{x} \tag{29}$$

$$\widetilde{a_{\mathcal{A}}}(\mathbf{u}, \tilde{\mathbf{u}}) \equiv 2\int_{\Omega_{\mathcal{A}}} \widetilde{\nu_{\mathcal{A}}}^H \mathbf{D}(\mathbf{u})^H : \nabla\tilde{\mathbf{u}}\, d\mathbf{x} + 2\int_{\Omega_{\mathcal{A}}} \widetilde{\nu_{\mathcal{A}}}^\perp \mathbf{D}(\mathbf{u})^\perp : \nabla\tilde{\mathbf{u}}\, d\mathbf{x} \tag{30}$$

$$a_{\mathcal{O}}(\mathbf{v}, \tilde{\mathbf{v}}) \equiv 2{\nu_{\mathcal{O}}}^H \int_{\Omega_{\mathcal{O}}} \mathbf{D}(\mathbf{v})^H : \nabla\tilde{\mathbf{v}}\, d\mathbf{x} + 2{\nu_{\mathcal{O}}}^\perp \int_{\Omega_{\mathcal{O}}} \mathbf{D}(\mathbf{v})^\perp : \nabla\tilde{\mathbf{v}}\, d\mathbf{x} \tag{31}$$

$$\widetilde{a_{\mathcal{O}}}(\mathbf{v}, \tilde{\mathbf{v}}) \equiv 2\int_{\Omega_{\mathcal{O}}} \widetilde{\nu_{\mathcal{O}}}^H \mathbf{D}(\mathbf{v})^H : \nabla\tilde{\mathbf{v}}\, d\mathbf{x} + 2\int_{\Omega_{\mathcal{O}}} \widetilde{\nu_{\mathcal{O}}}^\perp \mathbf{D}(\mathbf{v})^\perp : \nabla\tilde{\mathbf{v}}\, d\mathbf{x}. \tag{32}$$

Lemma 1. *Given functions* $(\tilde{\mathbf{u}}, \tilde{\mathbf{v}}) \in ((H^1(\Omega_{\mathcal{A}}))^d, (H^1(\Omega_{\mathcal{O}}))^d)$ *and* $(\mathbf{u}, \mathbf{v}) \in (V_{\mathcal{A}}, V_{\mathcal{O}})$, *it holds that*

$$a_{\mathcal{A}}(\mathbf{u}, \tilde{\mathbf{u}}) = {\nu_{\mathcal{A}}}^H \int_{\Omega_{\mathcal{A}}} (\nabla\mathbf{u})^H : (\nabla\tilde{\mathbf{u}})^H\, d\mathbf{x} + {\nu_{\mathcal{A}}}^\perp \int_{\Omega_{\mathcal{A}}} (\nabla\mathbf{u})^\perp : (\nabla\tilde{\mathbf{u}})^\perp\, d\mathbf{x}$$

$$a_{\mathcal{O}}(\mathbf{v}, \tilde{\mathbf{v}}) = {\nu_{\mathcal{O}}}^H \int_{\Omega_{\mathcal{O}}} (\nabla\mathbf{v})^H : (\nabla\tilde{\mathbf{v}})^H\, d\mathbf{x} + {\nu_{\mathcal{O}}}^\perp \int_{\Omega_{\mathcal{O}}} (\nabla\mathbf{v})^\perp : (\nabla\tilde{\mathbf{v}})^\perp\, d\mathbf{x}.$$

Proof. It suffices to take $\mathbf{u} \in \mathcal{C}^\infty(\overline{\Omega_{\mathcal{A}}}) \cap V_{\mathcal{A}}$ and $\mathbf{v} \in \mathcal{C}^\infty(\overline{\Omega_{\mathcal{O}}}) \cap V_{\mathcal{O}}$, since these subspaces are dense. Use the decomposition (7) and

$$(\nabla\mathbf{u})^H : (\nabla\tilde{\mathbf{u}})^\perp = 0 = (\nabla\tilde{\mathbf{u}})^H : (\nabla\mathbf{u})^\perp$$

to write

$$a_{\mathcal{A}}(\mathbf{u},\tilde{\mathbf{u}}) = 2{\nu_{\mathcal{A}}}^{H}\int_{\Omega_{\mathcal{A}}}\mathbf{D}(\mathbf{u})^{H} : \nabla\tilde{\mathbf{u}}\,d\mathbf{x} + 2{\nu_{\mathcal{A}}}^{\perp}\int_{\Omega_{\mathcal{A}}}\mathbf{D}(\mathbf{u})^{\perp} : \nabla\tilde{\mathbf{u}}\,d\mathbf{x}$$
$$= {\nu_{\mathcal{A}}}^{H}\int_{\Omega_{\mathcal{A}}}(\nabla\mathbf{u})^{H} : (\nabla\tilde{\mathbf{u}})^{H} + \left(\nabla\mathbf{u}^{T}\right)^{H} : (\nabla\tilde{\mathbf{u}})^{H}\,d\mathbf{x}$$
$$+ {\nu_{\mathcal{A}}}^{\perp}\int_{\Omega_{\mathcal{A}}}(\nabla\mathbf{u})^{\perp} : (\nabla\tilde{\mathbf{u}})^{\perp} + \left(\nabla\mathbf{u}^{T}\right)^{\perp} : (\nabla\tilde{\mathbf{u}})^{\perp}\,d\mathbf{x}.$$

Integrate by parts to show that for each $i = 1,\ldots,d$,

$$\sum_{j=1,\ldots,d}\int_{\Omega_{\mathcal{A}}}\partial_{x_i}u_j\partial_{x_j}\tilde{u}_i\,d\mathbf{x} = -\int_{\Omega_{\mathcal{A}}}\partial_{x_i}\left(\sum_{j=1,\ldots,d}\partial_{x_j}u_j\right)\tilde{u}_i\,d\mathbf{x} = 0,$$

since $\mathbf{u}\in V_{\mathcal{A}} \Rightarrow \nabla\cdot\mathbf{u} = 0$. It follows that

$${\nu_{\mathcal{A}}}^{H}\int_{\Omega_{\mathcal{A}}}\left(\nabla\mathbf{u}^{T}\right)^{H} : (\nabla\tilde{\mathbf{u}})^{H}\,d\mathbf{x} = 0 = {\nu_{\mathcal{A}}}^{\perp}\int_{\Omega_{\mathcal{A}}}\left(\nabla\mathbf{u}^{T}\right)^{\perp} : (\nabla\tilde{\mathbf{u}})^{\perp}\,d\mathbf{x},$$

and therefore

$$a_{\mathcal{A}}(\mathbf{u},\tilde{\mathbf{u}}) = {\nu_{\mathcal{A}}}^{H}\int_{\Omega_{\mathcal{A}}}(\nabla\mathbf{u})^{H} : (\nabla\tilde{\mathbf{u}})^{H}\,d\mathbf{x} + {\nu_{\mathcal{A}}}^{\perp}\int_{\Omega_{\mathcal{A}}}(\nabla\mathbf{u})^{\perp} : (\nabla\tilde{\mathbf{u}})^{\perp}\,d\mathbf{x}.$$

A similar analysis holds with $\mathbf{v}$ and $\tilde{\mathbf{v}}$. □

An application of the Poincarè-Friedrich inequality is used for the velocity spaces. The factor of 2 that appears in (34) below is for convenience in later application.

Lemma 2. *There exists a constant $\alpha_1 > 0$ such that*

$$\alpha_1\left\{\|\nabla\mathbf{u}\|^2 + \|\nabla\mathbf{v}\|^2\right\} \le a_{\mathcal{A}}(\mathbf{u},\mathbf{u}) + a_{\mathcal{O}}(\mathbf{v},\mathbf{v}), \tag{33}$$

for any $\mathbf{u}\in V_{\mathcal{A}}$ and $\mathbf{v}\in V_{\mathcal{O}}$. Furthermore, there exists a constant $\alpha_2 > 0$ such that

$$2\alpha_2\left\{\|\mathbf{u}\|^2 + \|\mathbf{v}\|^2\right\} \le \alpha_1\left\{\|\nabla\mathbf{u}\|^2 + \|\nabla\mathbf{v}\|^2\right\}, \tag{34}$$

for any $\mathbf{u}\in V_{\mathcal{A}}$ and $\mathbf{v}\in V_{\mathcal{O}}$.

Proof. It is clear from Lemma 1 that the constant α_1 can be defined by

$$\alpha_1 = \min\left\{{\nu_{\mathcal{A}}}^{H}, {\nu_{\mathcal{A}}}^{\perp}, {\nu_{\mathcal{O}}}^{H}, {\nu_{\mathcal{O}}}^{\perp}\right\}.$$

The rest follows from the observation that the Poincarè-Friedrich inequality holds on each domain $\Omega_{\mathcal{A}}$ and $\Omega_{\mathcal{O}}$. □

The polarization identity is useful to decompose vector products of the form $(\mathbf{u}-\mathbf{v})\cdot\mathbf{u}$ into positive and negative parts.

Lemma 3 (Polarization identity)**.** *Given equal-size vectors $\mathbf{u}$ and $\mathbf{v}$,*

$$2(\mathbf{u}-\mathbf{v})\cdot\mathbf{u} = |\mathbf{u}|^2 + |\mathbf{u}-\mathbf{v}|^2 - |\mathbf{v}|^2.$$

Ensembles of products can be manipulated using the next result to represent them in terms of fluctuations and ensemble averages.

Lemma 4 (Product ensemble identities)**.** *Given two sets of scalars a_j and b_j, $j = 1,\ldots,J$, it follows*

$$< a_j b_j > = < a_j' b_j' > + ab. \tag{35}$$

For two sets of vectors $\mathbf{a}_j$ and $\mathbf{b}_j$, $j = 1,\ldots,J$, it holds that

$$< \mathbf{a}_j\cdot\mathbf{b}_j > = < \mathbf{a}_j'\cdot\mathbf{b}_j' > + \mathbf{a}\cdot\mathbf{b}. \tag{36}$$

Proof. Since the averaging operator $< \cdot >$ distributes across addition and j-independent scalars can be pulled out,

$$\begin{aligned} < a_j b_j > &=< a'_j b'_j > + < a'_j b > + < a b'_j > + < ab > \\ &=< a'_j b'_j > + < a'_j > b + a < b'_j > + ab. \end{aligned}$$

Then (35) follows from noting that fluctuations average to zero;

$$< a'_j >=< b'_j >= 0.$$

The proof of (36) is similar. □

The following result will help later to study the effects of the nonlinear friction terms on the mean flow.

Lemma 5. *Given a set of vectors* $\mathbf{a}_j$*,* $j = 1, \ldots, J$*, it holds that*

$$\left\langle (|\mathbf{a}_j|\,\mathbf{a}_j)' \cdot \mathbf{a}'_j \right\rangle \geq 0.$$

Proof. Application of (36) gives

$$\begin{aligned} \left\langle (|\mathbf{a}_j|\,\mathbf{a}_j)' \cdot \mathbf{a}'_j \right\rangle &= \langle |\mathbf{a}_j|\,\mathbf{a}_j \cdot \mathbf{a}_j \rangle - \langle |\mathbf{a}_j|\,\mathbf{a}_j \rangle \cdot \langle \mathbf{a}_j \rangle \\ &= \left\langle |\mathbf{a}_j|^3 \right\rangle - \langle |\mathbf{a}_j|\,\mathbf{a}_j \rangle \cdot \langle \mathbf{a}_j \rangle . \end{aligned} \tag{37}$$

A lower bound may be found by first applying the Triangle and Minkowski inequalities to show that

$$\begin{aligned} |\langle |\mathbf{a}_j|\,\mathbf{a}_j \rangle| = \frac{1}{J} \left| \sum_{j=1}^{J} |\mathbf{a}_j|\,\mathbf{a}_j \right| &\leq \frac{1}{J} \sum_{j=1}^{J} |\mathbf{a}_j|^2 \leq \frac{1}{J} \left(\sum_{j=1}^{J} 1 \right)^{1/3} \left(\sum_{j=1}^{J} |\mathbf{a}_j|^3 \right)^{2/3} \\ &= \left(\frac{1}{J} \sum_{j=1}^{J} |\mathbf{a}_j|^3 \right)^{2/3} = \left\langle |\mathbf{a}_j|^3 \right\rangle^{2/3}. \end{aligned}$$

Similarly, it holds that

$$\begin{aligned} |\langle \mathbf{a}_j \rangle| = \frac{1}{J} \left| \sum_{j=1}^{J} \mathbf{a}_j \right| &\leq \frac{1}{J} \sum_{j=1}^{J} |\mathbf{a}_j| \leq \frac{1}{J} \left(\sum_{j=1}^{J} 1 \right)^{2/3} \left(\sum_{j=1}^{J} |\mathbf{a}_j|^3 \right)^{1/3} \\ &= \left(\frac{1}{J} \sum_{j=1}^{J} |\mathbf{a}_j|^3 \right)^{1/3} = \left\langle |\mathbf{a}_j|^3 \right\rangle^{1/3}. \end{aligned}$$

The desired lower bound in (37) follows from the above results, via Cauchy-Schwarz:

$$\begin{aligned} |\langle |\mathbf{a}_j|\,\mathbf{a}_j \rangle \cdot \langle \mathbf{a}_j \rangle| &\leq \left\langle |\mathbf{a}_j|^3 \right\rangle^{1/3} \left\langle |\mathbf{a}_j|^3 \right\rangle^{2/3} = \left\langle |\mathbf{a}_j|^3 \right\rangle \\ \Rightarrow \left\langle (|\mathbf{a}_j|\,\mathbf{a}_j)' \cdot \mathbf{a}'_j \right\rangle &\geq \left\langle |\mathbf{a}_j|^3 \right\rangle - \left\langle |\mathbf{a}_j|^3 \right\rangle = 0. \end{aligned}$$

□

The following monotonicity result is used later to analyze convergence of ensembles to statistical equilibrium.

Lemma 6 (Friction monotonicity)**.** *Define* $T : \mathbb{R}^d \to \mathbb{R}^d$ *by* $T(\mathbf{x}) = |\mathbf{x}|\mathbf{x}$*, for all* $\mathbf{x} \in \mathbb{R}^d$*,* $d \in \mathbb{N}$*. Then* $T \in \mathcal{C}^1(\mathbb{R}^d, \mathbb{R}^d)$ *and*

$$(T(\mathbf{x}) - T(\mathbf{y})) \cdot (\mathbf{x} - \mathbf{y}) \geq \frac{1}{4} |\mathbf{x} - \mathbf{y}|^3, \qquad \forall\, \mathbf{x}, \mathbf{y} \in \mathbb{R}^d. \tag{38}$$

Proof. At any point $\mathbf{x}$, the derivative $DT(\mathbf{x}) : \mathbb{R}^d \to \mathbb{R}^d$ is a linear map, defined for all arguments $\mathbf{y} \in \mathbb{R}^d$ by

$$DT(\mathbf{x})(\mathbf{y}) \equiv \begin{cases} 0, & \text{if } \mathbf{x} = 0 \\ \frac{\mathbf{x}\cdot\mathbf{y}}{|\mathbf{x}|}\mathbf{x} + |\mathbf{x}|\mathbf{y}, & \text{otherwise.} \end{cases} \tag{39}$$

It is a standard exercise in real analysis to verify this formula and that $T \in \mathcal{C}^1(\mathbb{R}^d, \mathbb{R}^d)$.

It remains to show (38) . Given two vectors $\mathbf{x}, \mathbf{y} \in \mathbb{R}^d$, define $\mathbf{a} = \mathbf{y} - \mathbf{x}$. Without loss of generality, $\mathbf{a} \neq 0$. One may write

$$(T(\mathbf{y}) - T(\mathbf{x})) \cdot (\mathbf{y} - \mathbf{x}) = \int_0^1 \frac{d}{ds} T(\mathbf{x} + s\mathbf{a}) \cdot \mathbf{a}\, ds = \int_0^1 DT(\mathbf{x} + s\mathbf{a})(\mathbf{a}) \cdot \mathbf{a}\, ds.$$

Note that $\mathbf{x} + s\mathbf{a} = 0$ is possible for at most one distinct value of s, so we may ignore this case in the above integral. It follows from (39) that

$$\begin{aligned} (T(\mathbf{y}) - T(\mathbf{x})) \cdot (\mathbf{y} - \mathbf{x}) &= \int_0^1 \frac{(\mathbf{x} + s\mathbf{a}) \cdot \mathbf{a}}{|\mathbf{x} + s\mathbf{a}|} (\mathbf{x} + s\mathbf{a}) \cdot \mathbf{a} + |\mathbf{x} + s\mathbf{a}| \mathbf{a} \cdot \mathbf{a}\, ds \\ &= \int_0^1 \frac{|(\mathbf{x} + s\mathbf{a}) \cdot \mathbf{a}|^2}{|\mathbf{x} + s\mathbf{a}|} + |\mathbf{x} + s\mathbf{a}||\mathbf{a}|^2\, ds \\ &\geq |\mathbf{a}|^2 \int_0^1 |\mathbf{x} + s\mathbf{a}|\, ds \geq \frac{1}{4}|\mathbf{a}|^3. \end{aligned}$$

The last inequality is equivalent to arguments in [11], page 131. □

Remark 2. *The value* $1/4$ *that appears in* (38) *is probably not sharp.*

3. Evolution of the model variance

Three sources of model uncertainties are considered: initial conditions, forcing terms and the friction parameters κ_j. Let $\|\cdot\|$ denote the standard L^2-norm; the domain is inferred by context. An arbitrary set of vector functions $\mathbf{w}_j$, $j = 1, \ldots, J$, are discussed on a generic domain.

Definition 7 (Variance)**.** The variances are given by

$$\begin{aligned} V(\mathbf{w}_j) &\equiv \left\langle \|\mathbf{w}_j\|^2 \right\rangle - \|\mathbf{w}\|^2, \\ V((\nabla \mathbf{w}_j)^H) &\equiv \left\langle \left\|(\nabla \mathbf{w}_j)^H\right\|^2 \right\rangle - \left\|(\nabla \mathbf{w})^H\right\|^2, \\ \text{and } \ V(\nabla \mathbf{w}_j^\perp) &\equiv \left\langle \left\|(\nabla \mathbf{w}_j)^\perp\right\|^2 \right\rangle - \left\|(\nabla \mathbf{w})^\perp\right\|^2. \end{aligned}$$

Note that the variance measures fluctuations:

Lemma 7.

$$\begin{aligned} V(\mathbf{w}_j) = \left\langle \left\|\mathbf{w}_j'\right\|^2 \right\rangle \geq 0, \quad V((\nabla \mathbf{w}_j)^H) = \left\langle \left\|((\nabla \mathbf{w}_j)^H)'\right\|^2 \right\rangle \geq 0, \\ V((\nabla \mathbf{w}_j)^\perp) = \left\langle \left\|((\nabla \mathbf{w}_j)^\perp)'\right\|^2 \right\rangle \geq 0. \end{aligned} \tag{40}$$

Proof. Let Ω denote the domain for $\mathbf{w}_j$. Apply (36) as follows:

$$\begin{aligned} \left\langle \|\mathbf{w}_j\|^2 \right\rangle &= \left\langle \int_\Omega \mathbf{w}_j \cdot \mathbf{w}_j\, d\mathbf{x} \right\rangle = \int_\Omega \langle \mathbf{w}_j \cdot \mathbf{w}_j \rangle\, d\mathbf{x} = \int_\Omega \langle \mathbf{w}_j' \cdot \mathbf{w}_j' \rangle\, d\mathbf{x} + \int_\Omega \mathbf{w} \cdot \mathbf{w}\, d\mathbf{x} \\ &= \left\langle \int_\Omega \left|\mathbf{w}_j'\right|^2\, d\mathbf{x} \right\rangle + \int_\Omega |\mathbf{w}|^2\, d\mathbf{x} = \langle \|\mathbf{w}_j'\|^2 \rangle + \|\mathbf{w}\|^2, \end{aligned}$$

which implies that

$$V(\mathbf{w}_j) = \left\langle \left\| \mathbf{w}_j' \right\|^2 \right\rangle.$$

The remainder of the proof is analogous. □

Given that strong model solutions exist for each realization, then an energy equality will be satisfied for each realization and for the mean flows. These equations can then be used to describe the evolution of the model variance.

Lemma 8. *Given strong solutions* $(\mathbf{u}_j, p_j)$ *and* $(\mathbf{v}_j, q_j)$ *to the model equations* (1)-(6) *with boundary conditions described above, the following energy equations are satisfied for* $j = 1, \ldots, J$*:*

$$\begin{aligned} (41) \qquad & \frac{d}{dt}\left\{ \|\mathbf{u}_j\|^2 + \frac{\rho_{\mathcal{O}}}{\rho_{\mathcal{A}}}\|\mathbf{v}_j\|^2 \right\} + a_{\mathcal{A}}(\mathbf{u}_j, \mathbf{u}_j) + \frac{\rho_{\mathcal{O}}}{\rho_{\mathcal{A}}} a_{\mathcal{O}}(\mathbf{v}_j, \mathbf{v}_j) \\ & + \int_{\Gamma_I} \kappa_j |\mathbf{u}_j - \mathbf{v}_j|^3 \, d\Gamma_I = \int_{\Omega_{\mathcal{A}}} \mathbf{f}_{\mathcal{A}j} \cdot \mathbf{u}_j \, d\mathbf{x} + \frac{\rho_{\mathcal{O}}}{\rho_{\mathcal{A}}} \int_{\Omega_{\mathcal{O}}} \mathbf{f}_{\mathcal{O}\,j} \cdot \mathbf{v}_j \, d\mathbf{x}, \\ (42) \qquad & \frac{d}{dt}\left\{ \|\mathbf{u}\|^2 + \frac{\rho_{\mathcal{O}}}{\rho_{\mathcal{A}}}\|\mathbf{v}\|^2 \right\} + \int_{\Gamma_I} \langle \kappa_j |\mathbf{u}_j - \mathbf{v}_j| (\mathbf{u}_j - \mathbf{v}_j) \rangle \cdot (\mathbf{u} - \mathbf{v}) \, d\Gamma_I \\ & + a_{\mathcal{A}}(\mathbf{u}, \mathbf{u}) + \frac{\rho_{\mathcal{O}}}{\rho_{\mathcal{A}}} a_{\mathcal{O}}(\mathbf{v}, \mathbf{v}) = \int_{\Omega_{\mathcal{A}}} \mathbf{f}_{\mathcal{A}} \cdot \mathbf{u} \, d\mathbf{x} + \frac{\rho_{\mathcal{O}}}{\rho_{\mathcal{A}}} \int_{\Omega_{\mathcal{O}}} \mathbf{f}_{\mathcal{O}} \cdot \mathbf{v} \, d\mathbf{x} \\ & - \int_{\Omega_{\mathcal{A}}} R(\mathbf{u}, \mathbf{u}) : \nabla \mathbf{u} \, d\mathbf{x} - \frac{\rho_{\mathcal{O}}}{\rho_{\mathcal{A}}} \int_{\Omega_{\mathcal{O}}} R(\mathbf{v}, \mathbf{v}) : \nabla \mathbf{v} \, d\mathbf{x}. \end{aligned}$$

Proof. Multiply through (1) by $\mathbf{u}_j$ and integrate over $\Omega_{\mathcal{A}}$. Also multiply through (4) by $\rho_{\mathcal{O}}\mathbf{v}_j/\rho_{\mathcal{A}}$ and integrate over $\Omega_{\mathcal{O}}$, adding the two equations together. Given the boundary condtions, it is easily shown that

$$\int_{\Omega_{\mathcal{A}}} \mathbf{u}_j \cdot \nabla \mathbf{u}_j \cdot \mathbf{u}_j \, d\mathbf{x} = \int_{\Omega_{\mathcal{O}}} \mathbf{v}_j \cdot \nabla \mathbf{v}_j \cdot \mathbf{v}_j \, d\mathbf{x} = 0 = \int_{\Omega_{\mathcal{A}}} \nabla p_j \cdot \mathbf{u}_j \, d\mathbf{x} = \int_{\Omega_{\mathcal{O}}} \nabla q_j \cdot \mathbf{v}_j \, d\mathbf{x}.$$

For the diffusion terms, note that

$$\begin{aligned} & - \int_{\Omega_{\mathcal{A}}} \mathcal{D}_{\mathcal{A}}(\mathbf{u}_j) \cdot \mathbf{u}_j \, d\mathbf{x} - \frac{\rho_{\mathcal{O}}}{\rho_{\mathcal{A}}} \int_{\Omega_{\mathcal{O}}} \mathcal{D}_{\mathcal{O}}(\mathbf{v}_j) \cdot \mathbf{v}_j \, d\mathbf{x} = a_{\mathcal{A}}(\mathbf{u}_j, \mathbf{u}_j) + \frac{\rho_{\mathcal{O}}}{\rho_{\mathcal{A}}} a_{\mathcal{O}}(\mathbf{v}_j, \mathbf{v}_j) \\ & \quad + \int_{\Gamma_I} \kappa_j |\mathbf{u}_j - \mathbf{v}_j| (\mathbf{u}_j - \mathbf{v}_j) \cdot \mathbf{u}_j \, d\Gamma_I - \int_{\Gamma_I} \kappa_j |\mathbf{u}_j - \mathbf{v}_j| (\mathbf{u}_j - \mathbf{v}_j) \cdot \mathbf{v}_j \, d\Gamma_I \\ & \qquad = a_{\mathcal{A}}(\mathbf{u}_j, \mathbf{u}_j) + \frac{\rho_{\mathcal{O}}}{\rho_{\mathcal{A}}} a_{\mathcal{O}}(\mathbf{v}_j, \mathbf{v}_j) + \int_{\Gamma_I} \kappa_j |\mathbf{u}_j - \mathbf{v}_j|^3 \, d\Gamma_I. \end{aligned}$$

The rest is standard to derive (41). For (42) one multiplies through (11) by $\mathbf{u}$ and through (14) by $\rho_{\mathcal{O}}\mathbf{v}/\rho_{\mathcal{A}}$. Then follow the above procedure, applying the ensemble-averaged boundary conditions. □

Theorem 1 (Variance evolution)**.** *Given an ensemble of strong model solutions, the model variance must satisfy the integral equation*

$$
\begin{aligned}
&V(\mathbf{u}_j(T)) + \frac{\rho_{\mathcal{O}}}{\rho_{\mathcal{A}}} V(\mathbf{v}_j(T)) + \int_0^T {\nu_{\mathcal{A}}}^H V((\nabla \mathbf{u}_j(T))^H)\, dt + \int_0^T {\nu_{\mathcal{A}}}^\perp V((\nabla \mathbf{u}_j(T))^\perp)\, dt \\
&+ \frac{\rho_{\mathcal{O}}}{\rho_{\mathcal{A}}} \int_0^T {\nu_{\mathcal{O}}}^H V((\nabla \mathbf{v}_j(T))^H)\, dt + \frac{\rho_{\mathcal{O}}}{\rho_{\mathcal{A}}} \int_0^T {\nu_{\mathcal{O}}}^\perp V((\nabla \mathbf{v}_j(T))^\perp)\, dt \\
&+ \int_0^T \int_{\Gamma_I} \left\langle \{\kappa_j |\mathbf{u}_j - \mathbf{v}_j| (\mathbf{u}_j - \mathbf{v}_j)\}' \cdot (\mathbf{u}_j - \mathbf{v}_j)' \right\rangle \, d\Gamma_I \, dt \\
&= V(\mathbf{u}_j^0) + \frac{\rho_{\mathcal{O}}}{\rho_{\mathcal{A}}} V(\mathbf{v}_j^0) + \int_0^T \int_{\Omega_{\mathcal{A}}} \left\langle \mathbf{f}_{\mathcal{A}_j}' \cdot \mathbf{u}_j' \right\rangle + \frac{\rho_{\mathcal{O}}}{\rho_{\mathcal{A}}} \int_0^T \int_{\Omega_{\mathcal{O}}} \left\langle \mathbf{f}_{\mathcal{O}_j}' \cdot \mathbf{v}_j' \right\rangle \\
&+ \int_0^T \int_{\Omega_{\mathcal{A}}} R(\mathbf{u}, \mathbf{u}) : \nabla \mathbf{u} \, d\mathbf{x} \, dt + \frac{\rho_{\mathcal{O}}}{\rho_{\mathcal{A}}} \int_0^T \int_{\Omega_{\mathcal{O}}} R(\mathbf{v}, \mathbf{v}) : \nabla \mathbf{v} \, d\mathbf{x} \, dt.
\end{aligned}
$$

Proof. Integrate (41)-(42) in time and take the ensemble-average of the realization energy equations. Subtracting this from the time-integral of the mean-flow energy equation and applying Definition 7 yields

$$
\begin{aligned}
&V(\mathbf{u}_j(T)) + \frac{\rho_{\mathcal{O}}}{\rho_{\mathcal{A}}} V(\mathbf{v}_j(T)) + \int_0^T {\nu_{\mathcal{A}}}^H V((\nabla \mathbf{u}_j(T))^H)\, dt + \int_0^T {\nu_{\mathcal{A}}}^\perp V((\nabla \mathbf{u}_j(T))^\perp)\, dt \\
&+ \frac{\rho_{\mathcal{O}}}{\rho_{\mathcal{A}}} \int_0^T {\nu_{\mathcal{O}}}^H V((\nabla \mathbf{v}_j(T))^H)\, dt + \frac{\rho_{\mathcal{O}}}{\rho_{\mathcal{A}}} \int_0^T {\nu_{\mathcal{O}}}^\perp V((\nabla \mathbf{v}_j(T))^\perp)\, dt \\
&+ \int_0^T \int_{\Gamma_I} \left\langle \kappa_j |\mathbf{u}_j - \mathbf{v}_j|^3 \right\rangle - \left\langle \kappa_j |\mathbf{u}_j - \mathbf{v}_j| (\mathbf{u}_j - \mathbf{v}_j) \right\rangle \cdot (\mathbf{u} - \mathbf{v}) \, d\Gamma_I \, dt \\
&= V(\mathbf{u}_j^0) + \frac{\rho_{\mathcal{O}}}{\rho_{\mathcal{A}}} V(\mathbf{v}_j^0) + \int_0^T \int_{\Omega_{\mathcal{A}}} \left(\left\langle \mathbf{f}_{\mathcal{A}j} \cdot \mathbf{u}_j \right\rangle - \mathbf{f}_{\mathcal{A}} \cdot \mathbf{u} \right) \, d\mathbf{x} \, dt \\
&+ \frac{\rho_{\mathcal{O}}}{\rho_{\mathcal{A}}} \int_0^T \int_{\Omega_{\mathcal{O}}} \left(\left\langle \mathbf{f}_{\mathcal{O}j} \cdot \mathbf{v}_j \right\rangle - \mathbf{f}_{\mathcal{O}} \cdot \mathbf{v} \right) \, d\mathbf{x} \, dt \\
&+ \int_0^T \int_{\Omega_{\mathcal{A}}} R(\mathbf{u}, \mathbf{u}) : \nabla \mathbf{u} \, d\mathbf{x} \, dt + \frac{\rho_{\mathcal{O}}}{\rho_{\mathcal{A}}} \int_0^T \int_{\Omega_{\mathcal{O}}} R(\mathbf{v}, \mathbf{v}) : \nabla \mathbf{v} \, d\mathbf{x} \, dt.
\end{aligned}
$$

Apply (36) to the forcing terms:

$$
\left\langle \mathbf{f}_{\mathcal{A}j} \cdot \mathbf{u}_j \right\rangle - \mathbf{f}_{\mathcal{A}} \cdot \mathbf{u} = \left\langle \mathbf{f}_{\mathcal{A}_j}' \cdot \mathbf{u}_j' \right\rangle \text{ and } \left\langle \mathbf{f}_{\mathcal{O}j} \cdot \mathbf{v}_j \right\rangle - \mathbf{f}_{\mathcal{O}} \cdot \mathbf{v} = \left\langle \mathbf{f}_{\mathcal{O}_j}' \cdot \mathbf{v}_j' \right\rangle.
$$

In order to handle the interface terms, set $\gamma_j = \kappa_j |\mathbf{u}_j - \mathbf{v}_j| (\mathbf{u}_j - \mathbf{v}_j)$ and $\mathbf{w}_j = \mathbf{u}_j - \mathbf{v}_j$. It holds that

$$
\begin{aligned}
&\int_0^T \int_{\Gamma_I} \left\langle \kappa_j |\mathbf{u}_j - \mathbf{v}_j|^3 \right\rangle - \left\langle \kappa_j |\mathbf{u}_j - \mathbf{v}_j| (\mathbf{u}_j - \mathbf{v}_j) \right\rangle \cdot (\mathbf{u} - \mathbf{v}) \, d\Gamma_I \, dt \\
&\qquad = \int_0^T \int_{\Gamma_I} \left\langle \gamma_j \cdot \mathbf{w}_j' \right\rangle \, d\Gamma_I \, dt = \int_0^T \int_{\Gamma_I} \left\langle \gamma_j' \cdot \mathbf{w}_j' \right\rangle \, d\Gamma_I \, dt.
\end{aligned}
$$

The last step holds since $\left\langle \gamma \cdot \mathbf{w}_j' \right\rangle = \gamma \cdot \left\langle \mathbf{w}_j' \right\rangle = 0$. The desired result follows by combining the above equations. □

As a corollary, it may be shown that when perturbations are only introduced through the initial conditions, the Reynolds stresses must have a dissipative effect on the mean flow. This yields a proof (under certain conditions) of the so-called *Boussinesq assumption* that partially motivates the closure models (20)-(21). This

analysis was performed in [10], but their analysis did not account for the extra coupling terms present with the atmosphere-ocean problem.

Corollary 1. *Assume strong realizations* $(\mathbf{u}_j, p_j)$ *and* $(\mathbf{v}_j, q_j)$ *exist and the forcing terms satisfy* $\mathbf{f}_{\mathcal{A}j} \in L^\infty(0,T;L^2(\Omega_\mathcal{A}))$ *and* $\mathbf{f}_{\mathcal{O}j} \in L^\infty(0,T;L^2(\Omega_\mathcal{O}))$*, for* $j = 1,\dots,J$*. If* $\kappa_j' = 0$ *and* $\mathbf{f}_{\mathcal{A}j}' = \mathbf{f}_{\mathcal{O}j}' = 0$ *for* $j = 1,\dots,J$*, then*

$$\liminf_{T\to\infty}\left\{\frac{1}{T}\int_0^T\int_{\Omega_\mathcal{A}} R(\mathbf{u},\mathbf{u}):\nabla\mathbf{u}\,d\mathbf{x}\,dt + \frac{\rho_\mathcal{O}}{\rho_\mathcal{A}}\frac{1}{T}\int_0^T\int_{\Omega_\mathcal{O}} R(\mathbf{v},\mathbf{v}):\nabla\mathbf{v}\,d\mathbf{x}\,dt\right\} \geq 0.$$

Proof. The assumptions on the forcing terms imply further that the variance satisfies $V(\mathbf{u}_j) \in L^\infty(0,T;L^2(\Omega_\mathcal{A}))$ and that $V(\mathbf{v}_j) \in L^\infty(0,T;L^2(\Omega_\mathcal{O}))$, for all j, by standard arguments. Since also $\kappa_j' = 0$ and $\mathbf{f}_{\mathcal{A}j}' = \mathbf{f}_{\mathcal{O}j}' = 0$, Theorem 1 implies that

$$\begin{aligned}
&V(\mathbf{u}_j(T)) + \frac{\rho_\mathcal{O}}{\rho_\mathcal{A}}V(\mathbf{v}_j(T)) + \int_0^T {\nu_\mathcal{A}}^H V((\nabla\mathbf{u}_j(T))^H)\,dt + \int_0^T {\nu_\mathcal{A}}^\perp V((\nabla\mathbf{u}_j(T))^\perp)\,dt\\
&+ \frac{\rho_\mathcal{O}}{\rho_\mathcal{A}}\int_0^T {\nu_\mathcal{O}}^H V((\nabla\mathbf{v}_j(T))^H)\,dt + \frac{\rho_\mathcal{O}}{\rho_\mathcal{A}}\int_0^T {\nu_\mathcal{O}}^\perp V((\nabla\mathbf{v}_j(T))^\perp)\,dt\\
&+ \int_0^T\int_{\Gamma_I} \kappa\left\langle\{|\mathbf{u}_j-\mathbf{v}_j|(\mathbf{u}_j-\mathbf{v}_j)\}'\cdot(\mathbf{u}_j-\mathbf{v}_j)'\right\rangle\,d\Gamma_I\,dt\\
&= V(\mathbf{u}_j^0) + \frac{\rho_\mathcal{O}}{\rho_\mathcal{A}}V(\mathbf{v}_j^0) + \int_0^T\int_{\Omega_\mathcal{A}} R(\mathbf{u},\mathbf{u}):\nabla\mathbf{u}\,d\mathbf{x}\,dt + \frac{\rho_\mathcal{O}}{\rho_\mathcal{A}}\int_0^T\int_{\Omega_\mathcal{O}} R(\mathbf{v},\mathbf{v}):\nabla\mathbf{v}\,d\mathbf{x}\,dt.
\end{aligned}$$

Multiply through by $1/T$ and note that

$$\frac{1}{T}V(\mathbf{u}_j(T)) = \mathcal{O}\left(\frac{1}{T}\right),\quad \frac{1}{T}V(\mathbf{v}_j(T)) = \mathcal{O}\left(\frac{1}{T}\right),$$
$$\frac{1}{T}V(\mathbf{u}_j^0) = \mathcal{O}\left(\frac{1}{T}\right),\quad \frac{1}{T}V(\mathbf{v}_j^0) = \mathcal{O}\left(\frac{1}{T}\right).$$

Also, taking $\mathbf{a}_j = \mathbf{u}_j - \mathbf{v}_j$ in Lemma 5 yields

$$\frac{1}{T}\int_0^T\int_{\Gamma_I} \kappa\left\langle\{|\mathbf{u}_j-\mathbf{v}_j|(\mathbf{u}_j-\mathbf{v}_j)\}'\cdot(\mathbf{u}_j-\mathbf{v}_j)'\right\rangle\,d\Gamma_I\,dt \geq 0.$$

The remaining variance terms are non-negative by Lemma 7. □

Remark 3. *It is expected that Corollary 1 would still hold if the data fluctuations* κ_j'*,* $\mathbf{f}_{\mathcal{A}j}'$ *and* $\mathbf{f}_{\mathcal{O}j}'$ *are small enough (in an appropriate sense), or vanish quickly enough as* $T\to\infty$*.*

4. Leray-regularized realizations and properties

The model realizations shall employ a Leray-type regularization. That is, the ensemble averaging operator $<\cdot>$ is assumed to have a smoothing effect on the mean flow, so that replacement of the convecting velocity in the nonlinear term of a realization will result in a regularized model, in the sense of Leray, [14, 15]. The realizations satisfy

$$\partial_t\mathbf{u}_j - \mathcal{D}_\mathcal{A}(\mathbf{u}_j) - {\mathcal{D}_\mathcal{A}}^T(\mathbf{u}_j) + \mathbf{u}\cdot\nabla\mathbf{u}_j + \nabla p_j = \mathbf{f}_{\mathcal{A}j} \text{ on } \Omega_\mathcal{A}\times(0,T], \tag{43}$$
$$\partial_t\mathbf{v}_j - \mathcal{D}_\mathcal{O}(\mathbf{v}_j) - {\mathcal{D}_\mathcal{O}}^T(\mathbf{v}_j) + \mathbf{v}\cdot\nabla\mathbf{v}_j + \nabla q_j = \mathbf{f}_{\mathcal{O}j} \text{ on } \Omega_\mathcal{O}\times(0,T]. \tag{44}$$

The notation for the realizations is reused here. The incompressibility, initial and boundary conditions are unchanged from before.

Note that upon taking the ensemble-average of (43)-(44) the mean flow satisfies

$$\begin{aligned} \partial_t \mathbf{u} - \mathcal{D}_{\mathcal{A}}(\mathbf{u}) - \mathcal{D}_{\mathcal{A}}{}^T(\mathbf{u}) + \mathbf{u}\cdot\nabla\mathbf{u} + \nabla p &= \mathbf{f}_{\mathcal{A}} \text{ on } \Omega_{\mathcal{A}}\times(0,T], \\ \partial_t \mathbf{v} - \mathcal{D}_{\mathcal{O}}(\mathbf{v}) - \mathcal{D}_{\mathcal{O}}{}^T(\mathbf{v}) + \mathbf{v}\cdot\nabla\mathbf{v} + \nabla q &= \mathbf{f}_{\mathcal{O}} \text{ on } \Omega_{\mathcal{O}}\times(0,T]. \end{aligned}$$

Comparison with (11)-(16) reveals that the mean flow for the Leray-regularized ensemble differs from that of the standard NSE model ensemble only due to the closures (20)-(21) for the Reynolds stress terms.

In ensemble calculations for this regularized model, matrices for the convection terms will not depend on the particular ensemble member. In practice, ensemble members would be advanced one time step in serial fashion, requiring one ensemble averaging (a negligible cost) plus the recomputation of convection terms once per time step. The matrix assembly cost is thus reduced significantly in proportion to the (possibly large) ensemble size, as compared with standard ensemble methods. The resulting savings in run time will depend on the particular implementation and is left to future study.

Remark 4. *The mean flow still satisfies* (19) *on* Γ_I*. This is not closed for the mean flow, so the realizations are a coupled system of* J *equations. Existence of unique, strong solutions is assumed herein, in order to discuss algorithmic ideas. A time-stepping method is applied later that decouples these equations numerically.*

Unique, strong solutions for the realization equations are assumed to exist hereafter and to satisfy the following variational problem. For $1 \le j \le J$, $(\mathbf{u}_j, p_j) : t \to (X_{\mathcal{A}}, P_{\mathcal{A}})$ and $(\mathbf{v}_j, q_j) : t \to (X_{\mathcal{O}}, P_{\mathcal{O}})$ satisfy (for a.e. $t \in (0,T]$)

$$\begin{aligned} (\partial_t \mathbf{u}_j, \widetilde{\mathbf{u}})_{\mathcal{A}} + (\mathbf{u}\cdot\nabla\mathbf{u}_j, \widetilde{\mathbf{u}})_{\mathcal{A}} + a_{\mathcal{A}}(\mathbf{u}_j, \widetilde{\mathbf{u}}) &+ \widetilde{a_{\mathcal{A}}}(\mathbf{u}_j, \widetilde{\mathbf{u}}) - (p_j, \nabla\cdot\widetilde{\mathbf{u}})_{\mathcal{A}} \\ +\kappa_j \int_{\Gamma_I} |\mathbf{u}_j - \mathbf{v}_j|(\mathbf{u}_j - \mathbf{v}_j)\cdot\widetilde{\mathbf{u}}\, d\Gamma_I &= (\mathbf{f}_{\mathcal{A}j}, \widetilde{\mathbf{u}})_{\mathcal{A}},\ \forall \widetilde{\mathbf{u}} \in X_{\mathcal{A}} \qquad (45) \\ (\nabla\cdot\mathbf{u}_j, \tilde{p})_{\mathcal{A}} &= 0,\ \forall \tilde{p} \in P_{\mathcal{A}}, \qquad (46) \\ (\partial_t \mathbf{v}_j, \widetilde{\mathbf{v}})_{\mathcal{O}} + (\mathbf{v}\cdot\nabla\mathbf{v}_j, \widetilde{\mathbf{v}})_{\mathcal{O}} + a_{\mathcal{O}}(\mathbf{v}_j, \widetilde{\mathbf{v}}) &+ \widetilde{a_{\mathcal{O}}}(\mathbf{v}_j, \widetilde{\mathbf{v}}) - (q_j, \nabla\cdot\widetilde{\mathbf{v}})_{\mathcal{O}} \\ -\frac{\rho_{\mathcal{A}}}{\rho_{\mathcal{O}}}\kappa_j \int_{\Gamma_I} |\mathbf{u}_j - \mathbf{v}_j|(\mathbf{u}_j - \mathbf{v}_j)\cdot\widetilde{\mathbf{v}}\, d\Gamma_I &= (\mathbf{f}_{\mathcal{O}j}, \widetilde{\mathbf{v}})_{\mathcal{O}},\ \forall \widetilde{\mathbf{v}} \in X_{\mathcal{O}} \qquad (47) \\ (\nabla\cdot\mathbf{v}_j, \tilde{q})_{\mathcal{O}} &= 0,\ \forall \tilde{q} \in P_{\mathcal{O}}, \qquad (48) \end{aligned}$$

with $\mathbf{u}_j(t=0) = \mathbf{u}_j^0$ and $\mathbf{v}_j(t=0) = \mathbf{v}_j^0$. Here, it is assumed also that $\nabla\cdot\mathbf{u}_j^0 = \nabla\cdot\mathbf{v}_j^0 = 0$ and that $\mathbf{u}_j \in L^4(0,T;X_{\mathcal{A}})$ and $\mathbf{v}_j \in L^4(0,T;X_{\mathcal{O}})$. The time derivatives satisfy $\partial_t\mathbf{u}_j \in L^2(0,T;X_{\mathcal{A}}{}^*)$ and $\partial_t\mathbf{v}_j \in L^2(0,T;X_{\mathcal{O}}{}^*)$. This way to define strong solutions is consistent with [13].

Lemma 9 (Long-time stability)**.** *Assume* $(\mathbf{u}_j, p_j)$*,* $(\mathbf{v}_j, q_j)$ *are strong solutions of the realization equations for* $1 \le j \le J$ *and let the turbulent viscosity coefficients be constants. If* $\mathbf{f}_{\mathcal{A}j} \in L^\infty(0,\infty;L^2(\Omega_{\mathcal{A}}))$ *and* $\mathbf{f}_{\mathcal{O}j} \in L^\infty(0,\infty;L^2(\Omega_{\mathcal{O}}))$*, then for*

$0 < t < \infty$,

$$\|\mathbf{u}_j(t)\|^2 + \frac{\rho_{\mathcal{O}}}{\rho_{\mathcal{A}}}\|\mathbf{v}_j(t)\|^2 + \alpha_1 \int_0^t e^{-\alpha_2(t-\tau)} \left\{ \|\nabla \mathbf{u}_j(\tau)\|^2 + \frac{\rho_{\mathcal{O}}}{\rho_{\mathcal{A}}}\|\nabla \mathbf{v}_j(\tau)\|^2 \right\} d\tau$$
$$+ 2\int_0^t e^{-\alpha_2(t-\tau)}\kappa_j \|(\mathbf{u}_j - \mathbf{v}_j)(\tau)\|_I^3 \, d\tau$$
$$\leq e^{-\alpha_2 t}\left\{ \|\mathbf{u}_j^0\|^2 + \frac{\rho_{\mathcal{O}}}{\rho_{\mathcal{A}}}\|\mathbf{v}_j^0\|^2 \right\}$$
$$+ \frac{1 - e^{-\alpha_2 t}}{(\alpha_2)^2}\left\{ \lim_{T\to\infty} \|\mathbf{f}_{\mathcal{A}j}\|_{\infty,2}^2 + \frac{\rho_{\mathcal{O}}}{\rho_{\mathcal{A}}} \lim_{T\to\infty} \|\mathbf{f}_{\mathcal{O}j}\|_{\infty,2}^2 \right\}.$$

It follows that $\mathbf{u}_j \in L^\infty(0,\infty; L^2(\Omega_{\mathcal{A}}))$ *and* $\mathbf{v}_j \in L^\infty(0,\infty; L^2(\Omega_{\mathcal{O}}))$.

Proof. Define $\mathbf{w}_j = \sqrt{\rho_{\mathcal{O}}}\mathbf{v}_j/\sqrt{\rho_{\mathcal{A}}}$. It follows from (45)-(48) that

$$\frac{1}{2}\frac{d}{dt}\left\{\|\mathbf{u}_j\|^2 + \|\mathbf{w}_j\|^2\right\} + a_{\mathcal{A}}(\mathbf{u}_j, \mathbf{u}_j) + \widetilde{a_{\mathcal{A}}}(\mathbf{u}_j, \mathbf{u}_j) + a_{\mathcal{O}}(\mathbf{w}_j, \mathbf{w}_j) + \widetilde{a_{\mathcal{O}}}(\mathbf{w}_j, \mathbf{w}_j)$$
$$+\kappa_j\|\mathbf{u}_j - \mathbf{v}_j\|_I^3 = (\mathbf{f}_{\mathcal{A}j}, \mathbf{u}_j)_{\mathcal{A}} + \frac{\rho_{\mathcal{O}}}{\rho_{\mathcal{A}}}(\mathbf{f}_{\mathcal{O}j}, \mathbf{v}_j)_{\mathcal{O}} \leq \|\mathbf{f}_{\mathcal{A}j}\|\|\mathbf{u}_j\| + \frac{\rho_{\mathcal{O}}}{\rho_{\mathcal{A}}}\|\mathbf{f}_{\mathcal{O}j}\|\|\mathbf{v}_j\|.$$

Since the turbulent viscosity parameters are constants, the analysis of Lemma 1 and Lemma 2 may be applied to show that

$$\widetilde{a_{\mathcal{A}}}(\mathbf{u}_j, \mathbf{u}_j) + \widetilde{a_{\mathcal{O}}}(\mathbf{w}_j, \mathbf{w}_j) \geq 0.$$

Bound the remaining viscous terms below by applying Lemma 2. The result is

$$\frac{1}{2}\frac{d}{dt}\left\{\|\mathbf{u}_j\|^2 + \|\mathbf{w}_j\|^2\right\} + \alpha_2\left\{\|\mathbf{u}_j\|^2 + \|\mathbf{w}_j\|^2\right\} + \frac{\alpha_1}{2}\left\{\|\nabla\mathbf{u}_j\|^2 + \|\nabla\mathbf{w}_j\|^2\right\}$$
$$+ \kappa_j\|\mathbf{u}_j - \mathbf{v}_j\|_I^3 \leq \|\mathbf{f}_{\mathcal{A}j}\|\|\mathbf{u}_j\| + \frac{\rho_{\mathcal{O}}}{\rho_{\mathcal{A}}}\|\mathbf{f}_{\mathcal{O}j}\|\|\mathbf{v}_j\|.$$

Bound the right-hand side above using Young's inequality:

$$\frac{1}{2}\frac{d}{dt}\left\{\|\mathbf{u}_j\|^2 + \|\mathbf{w}_j\|^2\right\} + \alpha_2\left\{\|\mathbf{u}_j\|^2 + \|\mathbf{w}_j\|^2\right\} + \frac{\alpha_1}{2}\left\{\|\nabla\mathbf{u}_j\|^2 + \|\nabla\mathbf{w}_j\|^2\right\}$$
$$+\kappa_j\|\mathbf{u}_j - \mathbf{v}_j\|_I^3 \leq \frac{1}{2\alpha_2}\left\{\|\mathbf{f}_{\mathcal{A}j}\|^2 + \frac{\rho_{\mathcal{O}}}{\rho_{\mathcal{A}}}\|\mathbf{f}_{\mathcal{O}j}\|^2\right\} + \frac{\alpha_2}{2}\left\{\|\mathbf{u}_j\|^2 + \|\mathbf{w}_j\|^2\right\}$$
$$\Rightarrow \frac{1}{2}\frac{d}{dt}\left\{\|\mathbf{u}_j\|^2 + \|\mathbf{w}_j\|^2\right\} + \frac{\alpha_2}{2}\left\{\|\mathbf{u}_j\|^2 + \|\mathbf{w}_j\|^2\right\} + \frac{\alpha_1}{2}\left\{\|\nabla\mathbf{u}_j\|^2 + \|\nabla\mathbf{w}_j\|^2\right\}$$
$$+\kappa_j\|\mathbf{u}_j - \mathbf{v}_j\|_I^3 \leq \frac{1}{2\alpha_2}\left\{\|\mathbf{f}_{\mathcal{A}j}\|^2 + \frac{\rho_{\mathcal{O}}}{\rho_{\mathcal{A}}}\|\mathbf{f}_{\mathcal{O}j}\|^2\right\}.$$

The remainder of the proof follows by using an integration factor. □

The next result is needed to discuss convergence to statistical equilibrium.

Lemma 10. *Let the mapping* $\tau \to e^{-\alpha_2(t-\tau)}f(\tau) \in L^1(0,t)$ *satisfy*

$$\int_0^t e^{-\alpha_2(t-\tau)}|f(\tau)|\, d\tau \leq C < \infty$$

for all $0 < t < \infty$, *where* $\alpha_2 > 0$ *and* $C > 0$ *are independent of* τ *and* t. *Given any* $g \in L^\infty(0,\infty)$ *such that* $\limsup_{t\to\infty}|g(t)| = 0$, *it holds that*

$$\limsup_{t\to\infty}\int_0^t e^{-\alpha_2(t-\tau)}|g(\tau)||f(\tau)|\, d\tau = 0.$$

Proof. Without loss of generality, assume $\|g\|_{L^\infty} > 0$. Let $\delta > 0$ be arbitrary. Given $0 < s < t$,

$$\int_0^t e^{-\alpha_2(t-\tau)}|g(\tau)||f(\tau)|\,d\tau \leq \|g\|_{L^\infty}e^{-\alpha_2(t-s)}\int_0^s e^{-\alpha_2(s-\tau)}|f(\tau)|\,d\tau$$
$$+ \sup_{s\leq\tau\leq t}|g(\tau)|\int_s^t e^{-\alpha_2(t-\tau)}|f(\tau)|\,d\tau \leq C\|g\|_{L^\infty}e^{-\alpha_2(t-s)} + C\sup_{s\leq\tau\leq t}|g(\tau)|.$$

Choose s so large that $\sup_{s\leq\tau\leq\infty}|g(\tau)| < \delta/(2C)$ and then choose any $t^*(\delta) > s$ so large that

$$e^{-\alpha_2(t-s)} \leq e^{-\alpha_2(t^*-s)} < \frac{\delta}{2C\|g\|_{L^\infty}},$$

for all $t \geq t^*$. It follows that

$$0 \leq \sup_{t\geq t^*}\int_0^t e^{-\alpha_2(t-\tau)}|g(\tau)||f(\tau)|\,d\tau < \delta,$$

which is the desired result. □

Theorem 2. *Let the turbulent viscosity coefficients be constants. Assume that for all $1 \leq j \leq J$, $\mathbf{f}_{\mathcal{A}j} \in L^\infty(0,\infty;L^2(\Omega_{\mathcal{A}}))$, $\mathbf{f}_{\mathcal{O}j} \in L^\infty(0,\infty;L^2(\Omega_{\mathcal{O}}))$ and also that*

$$\limsup_{t\to\infty}\|\mathbf{f}_{\mathcal{A}j}'(t)\| = \limsup_{t\to\infty}\|\mathbf{f}_{\mathcal{O}j}'(t)\| = \limsup_{t\to\infty}\kappa_j'(t) = 0. \tag{49}$$

Given $(\mathbf{u}_i, p_i)$, $(\mathbf{v}_i, q_i)$ and $(\mathbf{u}_j, p_j)$, $(\mathbf{v}_j, q_j)$ are any strong solutions of the realization equations with $1 \leq i, j \leq J$, it holds that

$$\limsup_{t\to\infty}\left\{\|(\mathbf{u}_i-\mathbf{u}_j)(t)\|^2 + \frac{\rho_{\mathcal{O}}}{\rho_{\mathcal{A}}}\|(\mathbf{v}_i-\mathbf{v}_j)(t)\|^2\right\} = 0 \tag{50}$$

and

$$\limsup_{t\to\infty}\int_0^t e^{-\alpha_2(t-\tau)}\left\{\|\nabla(\mathbf{u}_i-\mathbf{u}_j)(\tau)\|^2 + \frac{\rho_{\mathcal{O}}}{\rho_{\mathcal{A}}}\|\nabla(\mathbf{v}_i-\mathbf{v}_j)(\tau)\|^2\right\}d\tau = 0. \tag{51}$$

Proof. Define $\mathbf{a} = \mathbf{u}_i - \mathbf{u}_j$ and $\mathbf{b} = \mathbf{v}_i - \mathbf{v}_j$. It follows from (45)-(48) that

$$\frac{1}{2}\frac{d}{dt}\|\mathbf{a}\|^2 + \int_{\Gamma_I}\kappa_i|\mathbf{u}_i-\mathbf{v}_i|(\mathbf{u}_i-\mathbf{v}_i)\cdot\mathbf{a}\,d\Gamma_I - \int_{\Gamma_I}\kappa_j|\mathbf{u}_j-\mathbf{v}_j|(\mathbf{u}_j-\mathbf{v}_j)\cdot\mathbf{a}\,d\Gamma_I$$
$$+ a_{\mathcal{A}}(\mathbf{a},\mathbf{a}) + \widetilde{a_{\mathcal{A}}}(\mathbf{a},\mathbf{a}) = \left(\mathbf{f}_{\mathcal{A}i}-\mathbf{f}_{\mathcal{A}j},\mathbf{a}\right)_{\mathcal{A}}.$$

Next, decompose the data κ_i, κ_j, $\mathbf{f}_{\mathcal{A}i}$ and $\mathbf{f}_{\mathcal{A}j}$ in terms of fluctuations and means, then insert above and rearrange terms to see that

$$\frac{1}{2}\frac{d}{dt}\|\mathbf{a}\|^2 + \int_{\Gamma_I}\kappa|\mathbf{u}_i-\mathbf{v}_i|(\mathbf{u}_i-\mathbf{v}_i)\cdot\mathbf{a}\,d\Gamma_I - \int_{\Gamma_I}\kappa|\mathbf{u}_j-\mathbf{v}_j|(\mathbf{u}_j-\mathbf{v}_j)\cdot\mathbf{a}\,d\Gamma_I$$
$$+ a_{\mathcal{A}}(\mathbf{a},\mathbf{a}) + \widetilde{a_{\mathcal{A}}}(\mathbf{a},\mathbf{a}) = \left(\mathbf{f}_{\mathcal{A}i}'-\mathbf{f}_{\mathcal{A}j}',\mathbf{a}\right)_{\mathcal{A}}$$
$$- \int_{\Gamma_I}\kappa_i'|\mathbf{u}_i-\mathbf{v}_i|(\mathbf{u}_i-\mathbf{v}_i)\cdot\mathbf{a}\,d\Gamma_I + \int_{\Gamma_I}\kappa_j'|\mathbf{u}_j-\mathbf{v}_j|(\mathbf{u}_j-\mathbf{v}_j)\cdot\mathbf{a}\,d\Gamma_I.$$

On the domain $\Omega_{\mathcal{O}}$ an analogous equation is derived and added to the above result, which leads to

$$\begin{aligned}
&\frac{1}{2}\frac{d}{dt}\left\{\|\mathbf{a}\|^2+\frac{\rho_{\mathcal{O}}}{\rho_{\mathcal{A}}}\|\mathbf{b}\|^2\right\}+a_{\mathcal{A}}(\mathbf{a},\mathbf{a})+\widetilde{a_{\mathcal{A}}}(\mathbf{a},\mathbf{a})+\frac{\rho_{\mathcal{O}}}{\rho_{\mathcal{A}}}a_{\mathcal{O}}(\mathbf{b},\mathbf{b})+\frac{\rho_{\mathcal{O}}}{\rho_{\mathcal{A}}}\widetilde{a_{\mathcal{O}}}(\mathbf{b},\mathbf{b})\\
&+\int_{\Gamma_I}\kappa|\mathbf{u}_i-\mathbf{v}_i|(\mathbf{u}_i-\mathbf{v}_i)\cdot(\mathbf{a}-\mathbf{b})\,d\Gamma_I-\int_{\Gamma_I}\kappa|\mathbf{u}_j-\mathbf{v}_j|(\mathbf{u}_j-\mathbf{v}_j)\cdot(\mathbf{a}-\mathbf{b})\,d\Gamma_I\\
=&-\int_{\Gamma_I}\kappa_i'|\mathbf{u}_i-\mathbf{v}_i|(\mathbf{u}_i-\mathbf{v}_i)\cdot(\mathbf{a}-\mathbf{b})\,d\Gamma_I+\int_{\Gamma_I}\kappa_j'|\mathbf{u}_j-\mathbf{v}_j|(\mathbf{u}_j-\mathbf{v}_j)\cdot(\mathbf{a}-\mathbf{b})\,d\Gamma_I\\
&+\left(\mathbf{f}_{\mathcal{A}_i}'-\mathbf{f}_{\mathcal{A}_j}',\mathbf{a}\right)_{\mathcal{A}}+\frac{\rho_{\mathcal{O}}}{\rho_{\mathcal{A}}}\left(\mathbf{f}_{\mathcal{O}_i}'-\mathbf{f}_{\mathcal{O}_j}',\mathbf{b}\right)_{\mathcal{O}}.
\end{aligned}$$

The interface terms on the left are treated by applying the monotonicity result Lemma 6, with $\mathbf{x}=\mathbf{u}_i-\mathbf{v}_i$ and $\mathbf{y}=\mathbf{u}_j-\mathbf{v}_j$. Then $\mathbf{x}-\mathbf{y}=\mathbf{a}-\mathbf{b}$ and

$$\begin{aligned}
&\int_{\Gamma_I}\kappa|\mathbf{u}_i-\mathbf{v}_i|(\mathbf{u}_i-\mathbf{v}_i)\cdot(\mathbf{a}-\mathbf{b})\,d\Gamma_I-\int_{\Gamma_I}\kappa|\mathbf{u}_j-\mathbf{v}_j|(\mathbf{u}_j-\mathbf{v}_j)\cdot(\mathbf{a}-\mathbf{b})\,d\Gamma_I\\
&\quad=\int_{\Gamma_I}\kappa\left(|\mathbf{x}|\mathbf{x}-|\mathbf{y}|\mathbf{y}\right)\cdot(\mathbf{a}-\mathbf{b})\,d\Gamma_I=\int_{\Gamma_I}\kappa\left(|\mathbf{x}|\mathbf{x}-|\mathbf{y}|\mathbf{y}\right)\cdot(\mathbf{x}-\mathbf{y})\,d\Gamma_I\\
&\qquad\qquad\geq\frac{1}{4}\int_{\Gamma_I}\kappa\,|\mathbf{x}-\mathbf{y}|^3\,d\Gamma_I=\frac{1}{4}\int_{\Gamma_I}\kappa\,|\mathbf{a}-\mathbf{b}|^3\,d\Gamma_I\geq 0.
\end{aligned}$$

Next, bound the viscous terms below by applying Lemma 2. Upon combining the above results, it holds that

$$\begin{aligned}
(52)\ &\frac{1}{2}\frac{d}{dt}\left\{\|\mathbf{a}\|^2+\frac{\rho_{\mathcal{O}}}{\rho_{\mathcal{A}}}\|\mathbf{b}\|^2\right\}+\alpha_2\left\{\|\mathbf{a}\|^2+\frac{\rho_{\mathcal{O}}}{\rho_{\mathcal{A}}}\|\mathbf{b}\|^2\right\}\\
&+\frac{\alpha_1}{2}\left\{\|\nabla\mathbf{a}\|^2+\frac{\rho_{\mathcal{O}}}{\rho_{\mathcal{A}}}\|\nabla\mathbf{b}\|^2\right\}\leq\left(\|\mathbf{f}_{\mathcal{A}_i}'\|+\|\mathbf{f}_{\mathcal{A}_j}'\|\right)\|\mathbf{a}\|+\frac{\rho_{\mathcal{O}}}{\rho_{\mathcal{A}}}\left(\|\mathbf{f}_{\mathcal{O}_i}'\|+\|\mathbf{f}_{\mathcal{O}_j}'\|\right)\|\mathbf{b}\|\\
&+|\kappa_i'|\int_{\Gamma_I}|\mathbf{u}_i-\mathbf{v}_i|^2|\mathbf{a}-\mathbf{b}|\,d\Gamma_I+|\kappa_j'|\int_{\Gamma_I}|\mathbf{u}_j-\mathbf{v}_j|^2|\mathbf{a}-\mathbf{b}|\,d\Gamma_I.
\end{aligned}$$

Young's inequality is used to bound

$$\begin{aligned}
(53)\ &\left(\|\mathbf{f}_{\mathcal{A}_i}'\|+\|\mathbf{f}_{\mathcal{A}_j}'\|\right)\|\mathbf{a}\|+\frac{\rho_{\mathcal{O}}}{\rho_{\mathcal{A}}}\left(\|\mathbf{f}_{\mathcal{O}_i}'\|+\|\mathbf{f}_{\mathcal{O}_j}'\|\right)\|\mathbf{b}\|\\
&\leq\frac{2}{\alpha_2}\left\{\|\mathbf{f}_{\mathcal{A}_i}'\|^2+\|\mathbf{f}_{\mathcal{A}_j}'\|^2+\frac{\rho_{\mathcal{O}}}{\rho_{\mathcal{A}}}\|\mathbf{f}_{\mathcal{O}_i}'\|^2+\frac{\rho_{\mathcal{O}}}{\rho_{\mathcal{A}}}\|\mathbf{f}_{\mathcal{O}_j}'\|^2\right\}+\frac{\alpha_2}{2}\left\{\|\mathbf{a}\|^2+\frac{\rho_{\mathcal{O}}}{\rho_{\mathcal{A}}}\|\mathbf{b}\|^2\right\}.
\end{aligned}$$

The interface terms on the right of (52) require more work. First, note that

$$|\mathbf{a}-\mathbf{b}|=|\mathbf{x}-\mathbf{y}|\leq|\mathbf{u}_i-\mathbf{v}_i|+|\mathbf{u}_j-\mathbf{v}_j|.$$

It follows from Young's inequality that

$$\begin{aligned}
&|\kappa_i'|\int_{\Gamma_I}|\mathbf{u}_i-\mathbf{v}_i|^2|\mathbf{a}-\mathbf{b}|\,d\Gamma_I+|\kappa_j'|\int_{\Gamma_I}|\mathbf{u}_j-\mathbf{v}_j|^2|\mathbf{a}-\mathbf{b}|\,d\Gamma_I\\
&\leq\frac{5}{3}|\kappa_i'|\int_{\Gamma_I}|\mathbf{u}_i-\mathbf{v}_i|^3\,d\Gamma_I+\frac{5}{3}|\kappa_j'|\int_{\Gamma_I}|\mathbf{u}_j-\mathbf{v}_j|^3\,d\Gamma_I\\
&\quad+\frac{1}{3}|\kappa_i'|\int_{\Gamma_I}|\mathbf{u}_j-\mathbf{v}_j|^3\,d\Gamma_I+\frac{1}{3}|\kappa_j'|\int_{\Gamma_I}|\mathbf{u}_i-\mathbf{v}_i|^3\,d\Gamma_I.
\end{aligned}$$

Next, use the positivity requirement (18) to bound

$$
\begin{aligned}
&|\kappa_i'| \int_{\Gamma_I} |\mathbf{u}_i - \mathbf{v}_i|^2 |\mathbf{a} - \mathbf{b}| \, d\Gamma_I + |\kappa_j'| \int_{\Gamma_I} |\mathbf{u}_j - \mathbf{v}_j|^2 |\mathbf{a} - \mathbf{b}| \, d\Gamma_I \\
&\leq \frac{5|\kappa_i'| + |\kappa_j'|}{3\kappa_0} \kappa_i \int_{\Gamma_I} |\mathbf{u}_i - \mathbf{v}_i|^3 \, d\Gamma_I + \frac{5|\kappa_j'| + |\kappa_i'|}{3\kappa_0} \kappa_j \int_{\Gamma_I} |\mathbf{u}_j - \mathbf{v}_j|^3 \, d\Gamma_I.
\end{aligned}
$$

This result and (53) provide an upper bound for the right-hand side of (52). After some algebra, one obtains

$$
\begin{aligned}
&\frac{d}{dt} \left\{ \|\mathbf{a}\|^2 + \frac{\rho_{\mathcal{O}}}{\rho_{\mathcal{A}}} \|\mathbf{b}\|^2 \right\} + \alpha_2 \left\{ \|\mathbf{a}\|^2 + \frac{\rho_{\mathcal{O}}}{\rho_{\mathcal{A}}} \|\mathbf{b}\|^2 \right\} + \alpha_1 \left\{ \|\nabla \mathbf{a}\|^2 + \frac{\rho_{\mathcal{O}}}{\rho_{\mathcal{A}}} \|\nabla \mathbf{b}\|^2 \right\} \\
&\leq \frac{4}{\alpha_2} \left\{ \|\mathbf{f}_{\mathcal{A}_i}'\|^2 + \|\mathbf{f}_{\mathcal{A}_j}'\|^2 + \frac{\rho_{\mathcal{O}}}{\rho_{\mathcal{A}}} \|\mathbf{f}_{\mathcal{O}_i}'\|^2 + \frac{\rho_{\mathcal{O}}}{\rho_{\mathcal{A}}} \|\mathbf{f}_{\mathcal{O}_j}'\|^2 \right\} \\
&+ 2 \frac{5|\kappa_i'| + |\kappa_j'|}{3\kappa_0} \kappa_i \|\mathbf{u}_i - \mathbf{v}_i\|_I^3 + 2 \frac{5|\kappa_j'| + |\kappa_i'|}{3\kappa_0} \kappa_j \|\mathbf{u}_j - \mathbf{v}_j\|_I^3
\end{aligned}
$$

An integration factor may be used here to find that

$$
\begin{aligned}
&\|\mathbf{a}(t)\|^2 + \frac{\rho_{\mathcal{O}}}{\rho_{\mathcal{A}}} \|\mathbf{b}(t)\|^2 + \alpha_1 \int_0^t e^{-\alpha_2 (t-\tau)} \left\{ \|\nabla \mathbf{a}(\tau)\|^2 + \frac{\rho_{\mathcal{O}}}{\rho_{\mathcal{A}}} \|\nabla \mathbf{b}(\tau)\|^2 \right\} d\tau \\
&\leq e^{-\alpha_2 t} \left\{ \|\mathbf{a}(0)\|^2 + \frac{\rho_{\mathcal{O}}}{\rho_{\mathcal{A}}} \|\mathbf{b}(0)\|^2 \right\} \\
&+ \frac{4}{\alpha_2} \int_0^t e^{-\alpha_2 (t-\tau)} \left\{ \|\mathbf{f}_{\mathcal{A}_i}'\|^2 + \|\mathbf{f}_{\mathcal{A}_j}'\|^2 + \frac{\rho_{\mathcal{O}}}{\rho_{\mathcal{A}}} \|\mathbf{f}_{\mathcal{O}_i}'\|^2 + \frac{\rho_{\mathcal{O}}}{\rho_{\mathcal{A}}} \|\mathbf{f}_{\mathcal{O}_j}'\|^2 \right\} d\tau \\
&+ \frac{2}{3\kappa_0} \int_0^t e^{-\alpha_2 (t-\tau)} (5|\kappa_i'| + |\kappa_j'|) \kappa_i \|\mathbf{u}_i - \mathbf{v}_i\|_I^3 \, d\tau \\
&+ \frac{2}{3\kappa_0} \int_0^t e^{-\alpha_2 (t-\tau)} (5|\kappa_j'| + |\kappa_i'|) \kappa_j \|\mathbf{u}_j - \mathbf{v}_j\|_I^3 \, d\tau.
\end{aligned} \tag{54}
$$

Due to (49) and the boundedness of the data $\mathbf{f}_{\mathcal{A}j}$ and $\mathbf{f}_{\mathcal{O}j}$, it holds that

$$
\tau \to g_1(\tau) \equiv \|\mathbf{f}_{\mathcal{A}_i}'(\tau)\|^2 + \|\mathbf{f}_{\mathcal{A}_j}'(\tau)\|^2 + \frac{\rho_{\mathcal{O}}}{\rho_{\mathcal{A}}} \|\mathbf{f}_{\mathcal{O}_i}'(\tau)\|^2 + \frac{\rho_{\mathcal{O}}}{\rho_{\mathcal{A}}} \|\mathbf{f}_{\mathcal{O}_j}'(\tau)\|^2 \in L^\infty(0, \infty)
$$

such that $\limsup_{\tau \to \infty} |g_1(\tau)| = 0$. Therefore, Lemma 10 may be applied with $g = g_1$ and $f(\tau) = 1$ to show that

$$
\limsup_{t \to \infty} \int_0^t e^{-\alpha_2 (t-\tau)} \left\{ \|\mathbf{f}_{\mathcal{A}_i}'\|^2 + \|\mathbf{f}_{\mathcal{A}_j}'\|^2 + \frac{\rho_{\mathcal{O}}}{\rho_{\mathcal{A}}} \|\mathbf{f}_{\mathcal{O}_i}'\|^2 + \frac{\rho_{\mathcal{O}}}{\rho_{\mathcal{A}}} \|\mathbf{f}_{\mathcal{O}_j}'\|^2 \right\} d\tau = 0.
$$

In order to show that the interface terms also vanish in the limit, first note that due to Lemma 9, for any $1 \leq j \leq J$

$$
\tau \to f(\tau) \equiv e^{-\alpha_2 (t-\tau)} \kappa_j(\tau) \|(\mathbf{u}_j - \mathbf{v}_j)(\tau)\|_I^3
$$

satisfies the assumptions of Lemma 10. Due to (49) and the uniform boundedness of the data κ_i and κ_j, it then follows from Lemma 10 that

$$
\begin{aligned}
&\limsup_{t \to \infty} \int_0^t e^{-\alpha_2 (t-\tau)} (5|\kappa_i'| + |\kappa_j'|) \kappa_i \|\mathbf{u}_i - \mathbf{v}_i\|_I^3 \, d\tau \\
&\qquad = \limsup_{t \to \infty} \int_0^t e^{-\alpha_2 (t-\tau)} (5|\kappa_j'| + |\kappa_i'|) \kappa_j \|\mathbf{u}_j - \mathbf{v}_j\|_I^3 \, d\tau = 0.
\end{aligned}
$$

The desired results are now evident from (54). □

5. Numerical methods and variance analysis

CTM realizations are to be computed using three methods that differ only in the treatment of the coupling across the interface. One method uses implicit coupling of velocities, called the *monolithic* method, which is analogous to solving atmosphere and ocean equations simultaneously as one large system. In practice, *partitioned* methods are commonly used, which decouple the velocities for the atmosphere and ocean systems. Monolithic coupling is used here only to provide a benchmark point of comparison for the partitioned methods.

The partitioned methods are based on the work by Connors, Howell and Layton [5], and they provide unconditional numerical stability. The proof of stability is omitted for brevity, but it is a simple consequence of combining [10], Theorem 4.6 and [5], Lemma 3.1. However, with a partitioned method the friction does not automatically satisfy the monotonicity property (see Lemma 6), which may inhibit convergence to equilibrium. For comparison, one of the two partitioned variants calculates the friction based on the approximation

$$\kappa_j|\mathbf{u}_j-\mathbf{v}_j|(\mathbf{u}_j-\mathbf{v}_j)\approx\kappa_j|\mathbf{u}-\mathbf{v}|(\mathbf{u}_j-\mathbf{v}_j),$$

which changes the mean flow and realizations, but is proved to guarantee convergence to statistical equilibrium.

5.1. Numerical methods to approximate realizations. Let $\Omega_{\mathcal{A}}$ and $\Omega_{\mathcal{O}}$ have associated conforming, triangular or tetrahedral meshes with mesh sizes $h_{\mathcal{A}}$ and $h_{\mathcal{O}}$, respectively, defined as the maximum diameter of a mesh element. Conforming finite element spaces are defined by using Taylor-Hood pairs, resulting in spaces $(\widetilde{X}_{\mathcal{A}},\widetilde{P}_{\mathcal{A}})$ and $(\widetilde{X}_{\mathcal{O}},\widetilde{P}_{\mathcal{O}})$. These elements are known to satisfy the so-called inf-sup or LBB condition (see [7, 2]) and have enjoyed wide-spread use for fluid computations. A uniform time step is used with size $\Delta t>0$. Given a function $g(t)\in C[0,\infty)$, let $g^n\approx g(t^n=n\Delta t)$ denote an approximation at the discrete time levels $n=0,1,\ldots$. Define explicitly skew-symmetrized trilinear forms for the convection terms by

$$c_{\mathcal{A}}(\mathbf{u},\mathbf{u}_j;\tilde{\mathbf{u}})\equiv\frac{1}{2}\int_{\Omega_{\mathcal{A}}}\mathbf{u}\cdot\nabla\mathbf{u}_j\cdot\tilde{\mathbf{u}}\,d\mathbf{x}-\frac{1}{2}\int_{\Omega_{\mathcal{A}}}\mathbf{u}\cdot\nabla\tilde{\mathbf{u}}\cdot\mathbf{u}_j\,d\mathbf{x}$$

and

$$c_{\mathcal{O}}(\mathbf{v},\mathbf{v}_j;\tilde{\mathbf{v}})\equiv\frac{1}{2}\int_{\Omega_{\mathcal{O}}}\mathbf{v}\cdot\nabla\mathbf{v}_j\cdot\tilde{\mathbf{v}}\,d\mathbf{x}-\frac{1}{2}\int_{\Omega_{\mathcal{O}}}\mathbf{v}\cdot\nabla\tilde{\mathbf{v}}\cdot\mathbf{v}_j\,d\mathbf{x}.$$

Define functions μ_j^n and $\overline{\mu}_j^n$ on Γ_I by

$$\mu_j^n\equiv\kappa_j(t^n)|\mathbf{u}_j^n-\mathbf{v}_j^n|\qquad\text{and}\qquad\overline{\mu}_j^n\equiv\kappa_j(t^n)|\mathbf{u}^n-\mathbf{v}^n|,$$

for $1\le j\le J$ and all n. The three coupling approaches are referred to as M (monolithic) and then P1 and P2 (partitioned). The friction terms are defined as follows.

$$\mathcal{I}_{\mathcal{A}}\left(\mathbf{u}_j^{n+1},\mathbf{v}_j^{n+1},\mathbf{u}_j^n,\mathbf{v}_j^n\right)=\begin{cases}\mu_j^{n+1}\left(\mathbf{u}_j^{n+1}-\mathbf{v}_j^{n+1}\right) & \text{(M)}\\ \sqrt{\mu_j^n}\left(\sqrt{\mu_j^n}\mathbf{u}_j^{n+1}-\sqrt{\mu_j^{n-1}}\mathbf{v}_j^n\right) & \text{(P1)}\\ \sqrt{\overline{\mu}_j^n}\left(\sqrt{\overline{\mu}_j^n}\mathbf{u}_j^{n+1}-\sqrt{\overline{\mu}_j^{n-1}}\mathbf{v}_j^n\right) & \text{(P2)}\end{cases}$$

$$\mathcal{I}_{\mathcal{O}}\left(\mathbf{u}_j^{n+1},\mathbf{v}_j^{n+1},\mathbf{u}_j^n,\mathbf{v}_j^n\right)=\begin{cases}\mu_j^{n+1}\left(\mathbf{v}_j^{n+1}-\mathbf{u}_j^{n+1}\right) & \text{(M)}\\ \sqrt{\mu_j^n}\left(\sqrt{\mu_j^n}\mathbf{v}_j^{n+1}-\sqrt{\mu_j^{n-1}}\mathbf{u}_j^n\right) & \text{(P1)}\\ \sqrt{\overline{\mu}_j^n}\left(\sqrt{\overline{\mu}_j^n}\mathbf{v}_j^{n+1}-\sqrt{\overline{\mu}_j^{n-1}}\mathbf{u}_j^n\right) & \text{(P2)}\end{cases}$$

TABLE 2. Choices for turbulent mixing lengths and turbulent energies.

	$\widetilde{\nu_{\mathcal{A}}}^H$	$\widetilde{\nu_{\mathcal{A}}}^\perp$
l	$\Delta t < \lvert(E(\mathbf{u}_j^H)^{n+1})'\rvert >$	$\Delta t < \lvert(E(\mathbf{u}_j^\perp)^{n+1})'\rvert >$
k'	$\frac{\rho_{\mathcal{A}}}{2} < \lvert(E(\mathbf{u}_j^H)^{n+1})'\rvert^2 >$	$\frac{\rho_{\mathcal{A}}}{2} < \lvert(E(\mathbf{u}_j^\perp)^{n+1})'\rvert^2 >$
	$\widetilde{\nu_{\mathcal{O}}}^H$	$\widetilde{\nu_{\mathcal{O}}}^\perp$
l	$\Delta t < \lvert(E(\mathbf{v}_j^H)^{n+1})'\rvert >$	$\Delta t < \lvert(E(\mathbf{v}_j^\perp)^{n+1})'\rvert >$
k'	$\frac{\rho_{\mathcal{O}}}{2} < \lvert(E(\mathbf{v}_j^H)^{n+1})'\rvert^2 >$	$\frac{\rho_{\mathcal{O}}}{2} < \lvert(E(\mathbf{v}_j^\perp)^{n+1})'\rvert^2 >$

Note that the coupling is linearized with both methods. Also, extrapolation is used to linearize the convecting velocity for efficiency. To this end, given numbers g^n, $n = 0, 1, \ldots$, define $E(g)^{n+1} \equiv 2g^n - g^{n-1}$. Then numerical approximations for the realizations are sought by finding $(\mathbf{u}_j^n, p_j^n) \in (\widetilde{X}_{\mathcal{A}}, \widetilde{P}_{\mathcal{A}})$ and $(\mathbf{v}_j^n, q_j^n) \in (\widetilde{X}_{\mathcal{O}}, \widetilde{P}_{\mathcal{O}})$ satisfying

$$
\begin{aligned}
&\frac{1}{2\Delta t}\left(3\mathbf{u}_j^{n+1} - 4\mathbf{u}_j^n + \mathbf{u}_j^{n-1}, \widetilde{\mathbf{u}}\right)_{\mathcal{A}} + c_{\mathcal{A}}(E(\mathbf{u})^{n+1}, \mathbf{u}_j^{n+1}, \widetilde{\mathbf{u}}) \\
&+ a_{\mathcal{A}}(\mathbf{u}_j^{n+1}, \widetilde{\mathbf{u}}) + \widetilde{a_{\mathcal{A}}}(\mathbf{u}_j^{n+1}, \widetilde{\mathbf{u}}) - (p_j^{n+1}, \nabla \cdot \widetilde{\mathbf{u}})_{\mathcal{A}} \\
&+ \int_{\Gamma_I} \mathcal{I}_{\mathcal{A}}\left(\mathbf{u}_j^{n+1}, \mathbf{v}_j^{n+1}, \mathbf{u}_j^n, \mathbf{v}_j^n\right) \cdot \widetilde{\mathbf{u}}\, d\Gamma_I \\
&+ \gamma_{\mathcal{A}}\left(\nabla \cdot \mathbf{u}_j^{n+1}, \nabla \cdot \widetilde{\mathbf{u}}\right)_{\mathcal{A}} = (\mathbf{f}_{\mathcal{A}}{}_j^{n+1}, \widetilde{\mathbf{u}})_{\mathcal{A}},\ \forall \widetilde{\mathbf{u}} \in \widetilde{X}_{\mathcal{A}} \\
&(\nabla \cdot \mathbf{u}_j^{n+1}, \tilde{p})_{\mathcal{A}} = 0,\ \forall \tilde{p} \in \widetilde{P}_{\mathcal{A}},
\end{aligned}
\tag{55}
$$

$$
\begin{aligned}
&\frac{1}{2\Delta t}(3\mathbf{v}_j^{n+1} - 4\mathbf{v}_j^n + \mathbf{v}_j^{n-1}, \widetilde{\mathbf{v}})_{\mathcal{O}} + c_{\mathcal{O}}(E(\mathbf{v})^{n+1}, \mathbf{v}_j^{n+1}, \widetilde{\mathbf{v}}) \\
&+ \frac{\rho_{\mathcal{A}}}{\rho_{\mathcal{O}}} \int_{\Gamma_I} \mathcal{I}_{\mathcal{O}}\left(\mathbf{u}_j^{n+1}, \mathbf{v}_j^{n+1}, \mathbf{u}_j^n, \mathbf{v}_j^n\right) \cdot \widetilde{\mathbf{v}}\, d\Gamma_I \\
&+ a_{\mathcal{O}}(\mathbf{v}_j^{n+1}, \widetilde{\mathbf{v}}) + \widetilde{a_{\mathcal{O}}}(\mathbf{v}_j^{n+1}, \widetilde{\mathbf{v}}) - (q_j^{n+1}, \nabla \cdot \widetilde{\mathbf{v}})_{\mathcal{O}} \\
&+ \gamma_{\mathcal{O}}\left(\nabla \cdot \mathbf{v}_j^{n+1}, \nabla \cdot \widetilde{\mathbf{v}}\right)_{\mathcal{O}} = (\mathbf{f}_{\mathcal{O}}{}_j^{n+1}, \widetilde{\mathbf{v}})_{\mathcal{O}},\ \forall \widetilde{\mathbf{v}} \in \widetilde{X}_{\mathcal{O}} \\
&(\nabla \cdot \mathbf{v}_j^{n+1}, \tilde{q})_{\mathcal{O}} = 0,\ \forall \tilde{q} \in \widetilde{P}_{\mathcal{O}},
\end{aligned}
\tag{56}
$$

with initial data $\mathbf{u}_j^0 \in \widetilde{X}_{\mathcal{A}}$ and $\mathbf{v}_j^0 \in \widetilde{X}_{\mathcal{O}}$. The constants $\gamma_{\mathcal{A}} > 0$ and $\gamma_{\mathcal{O}} > 0$ are known as "grad-div stabilization parameters" and help to improve mass conservation (see *e.g.* [3, 19]), since Taylor-Hood elements do not admit a divergence-free velocity space. Values for these parameters are to be determined by experiment. The turbulent viscosity coefficients are chosen as shown in Table 2.

Note that the coefficients for these linear systems do not depend on j except for the terms for the flux coupling over Γ_I. But these latter terms only affect a relatively small number of the total matrix entries. Furthermore, the partitioned methods are linearized; compared to nonlinear methods applied to the true realization equations, the approach in this paper is very fast to run.

5.2. Evolution of variance for the methods. In order to simplify the analysis in this section, variance is only introduced through the initial conditions. In general, it is expected that the variance for the discrete approximations M and P2 will vanish as time evolves so long as the fluctuations κ_j', $\mathbf{f}_{\mathcal{A}}{}_j'$ and $\mathbf{f}_{\mathcal{O}}{}_j'$ vanish fast enough in time. However, for method P1 this behavior may be inhibited and it is not known if the variance vanishes at long times.

Lemma 11. *Let $\kappa_j = \kappa > 0$ for all $j = 1, \ldots, J$. For methods M and P2, there exist numbers $R^n \geq 0$ and $S^n \geq 0$ for $n = 1, \ldots, N$, which depend on the method, such that*

$$\begin{aligned} &\int_{\Gamma_I} \left\langle \mathcal{I}_{\mathcal{A}} \left(\mathbf{u}_j^{n+1}, \mathbf{v}_j^{n+1}, \mathbf{u}_j^n, \mathbf{v}_j^n\right) \cdot \left(\mathbf{u}_j^{n+1}\right)' \right\rangle d\Gamma_I \\ &+ \int_{\Gamma_I} \left\langle \mathcal{I}_{\mathcal{O}} \left(\mathbf{u}_j^{n+1}, \mathbf{v}_j^{n+1}, \mathbf{u}_j^n, \mathbf{v}_j^n\right) \cdot \left(\mathbf{v}_j^{n+1}\right)' \right\rangle d\Gamma_I \\ &= S^{n+1} + R^{n+1} - R^n, \ n = 1, \ldots, N-1. \end{aligned} \tag{57}$$

Proof. Define $S^1 = 0$ for both methods. For method M, the relevant coupling terms satisfy

$$\begin{aligned} &\int_{\Gamma_I} \left\langle \mu_j^{n+1} \left(\mathbf{u}_j^{n+1} - \mathbf{v}_j^{n+1}\right) \cdot \left(\mathbf{u}_j^{n+1}\right)' \right\rangle d\Gamma_I - \int_{\Gamma_I} \left\langle \mu_j^{n+1} \left(\mathbf{u}_j^{n+1} - \mathbf{v}_j^{n+1}\right) \cdot \left(\mathbf{v}_j^{n+1}\right)' \right\rangle d\Gamma_I \\ &= \kappa \int_{\Gamma_I} \left\langle \left|\mathbf{u}_j^{n+1} - \mathbf{v}_j^{n+1}\right| \left(\mathbf{u}_j^{n+1} - \mathbf{v}_j^{n+1}\right) \cdot \left(\mathbf{u}_j^{n+1} - \mathbf{v}_j^{n+1}\right)' \right\rangle d\Gamma_I \\ &= \kappa \int_{\Gamma_I} \left\langle \left\{ \left|\mathbf{u}_j^{n+1} - \mathbf{v}_j^{n+1}\right| \left(\mathbf{u}_j^{n+1} - \mathbf{v}_j^{n+1}\right) \right\}' \cdot \left(\mathbf{u}_j^{n+1} - \mathbf{v}_j^{n+1}\right)' \right\rangle d\Gamma_I. \end{aligned}$$

It follows from Lemma 5 that

$$\kappa \int_{\Gamma_I} \left\langle \left\{ \left|\mathbf{u}_j^{n+1} - \mathbf{v}_j^{n+1}\right| \left(\mathbf{u}_j^{n+1} - \mathbf{v}_j^{n+1}\right) \right\}' \cdot \left(\mathbf{u}_j^{n+1} - \mathbf{v}_j^{n+1}\right)' \right\rangle d\Gamma_I \equiv S^{n+1} \geq 0$$

for $n = 1, \ldots, N-1$. For method M, take $R^n = 0$ for all n.

Note that for method P2, the numbers $\overline{\mu}_j^n$ satisfy $\overline{\mu}_j^n = \kappa(t^n)|\mathbf{u}^n - \mathbf{v}^n|$, which does not depend on j. Then the interface terms satisfy

$$\begin{aligned} &\int_{\Gamma_I} \left\langle \left(\sqrt{\overline{\mu}_j^n} \mathbf{u}_j^{n+1} - \sqrt{\overline{\mu}_j^{n-1}} \mathbf{v}_j^n \right) \cdot \left(\sqrt{\overline{\mu}_j^n} \mathbf{u}_j^{n+1} \right)' \right\rangle d\Gamma_I \\ &+ \int_{\Gamma_I} \left\langle \left(\sqrt{\overline{\mu}_j^n} \mathbf{v}_j^{n+1} - \sqrt{\overline{\mu}_j^{n-1}} \mathbf{u}_j^n \right) \cdot \left(\sqrt{\overline{\mu}_j^n} \mathbf{v}_j^{n+1} \right)' \right\rangle d\Gamma_I \\ &= \int_{\Gamma_I} \left\langle \left\{ \left(\sqrt{\overline{\mu}_j^n} \mathbf{u}_j^{n+1} \right)' - \left(\sqrt{\overline{\mu}_j^{n-1}} \mathbf{v}_j^n \right)' \right\} \cdot \left(\sqrt{\overline{\mu}_j^n} \mathbf{u}_j^{n+1} \right)' \right\rangle d\Gamma_I \\ &+ \int_{\Gamma_I} \left\langle \left\{ \left(\sqrt{\overline{\mu}_j^n} \mathbf{v}_j^{n+1} \right)' - \left(\sqrt{\overline{\mu}_j^{n-1}} \mathbf{u}_j^n \right)' \right\} \cdot \left(\sqrt{\overline{\mu}_j^n} \mathbf{v}_j^{n+1} \right)' \right\rangle d\Gamma_I. \end{aligned}$$

The polarization identity may be applied to write the above terms in the form $S^{n+1} + R^{n+1} - R^n$, where

$$\begin{aligned} R^{n+1} &= \frac{1}{2} \int_{\Gamma_I} \overline{\mu}_j^n \left\langle \left| \left(\mathbf{u}_j^{n+1}\right)' \right|^2 \right\rangle + \overline{\mu}_j^n \left\langle \left| \left(\mathbf{v}_j^{n+1}\right)' \right|^2 \right\rangle d\Gamma_I \geq 0, \\ S^{n+1} &= \frac{1}{2} \int_{\Gamma_I} \left\langle \left| \sqrt{\overline{\mu}_j^n} \left(\mathbf{u}_j^{n+1}\right)' - \sqrt{\overline{\mu}_j^{n-1}} \left(\mathbf{v}_j^n\right)' \right|^2 \right\rangle d\Gamma_I \\ &\quad + \frac{1}{2} \int_{\Gamma_I} \left\langle \left| \sqrt{\overline{\mu}_j^n} \left(\mathbf{v}_j^{n+1}\right)' - \sqrt{\overline{\mu}_j^{n-1}} \left(\mathbf{u}_j^n\right)' \right|^2 \right\rangle d\Gamma_I \geq 0. \end{aligned}$$

□

It can be shown that Lemma 11 need not hold in a purely algebraic sense for method P1. As a result, spurious variance might be created numerically for method P1 through the coupling terms and inhibit convergence to statistical equilibrium.

Theorem 3. *Let the turbulent viscosities be constants. Assume* $\kappa_j' = 0$, $\mathbf{f}_{\mathcal{A}j}' = 0$ *and* $\mathbf{f}_{\mathcal{O}j}' = 0$ *identically, for all* j. *Then the discrete solutions for methods M and P2 satisfy*

$$\lim_{n\to\infty}\left(V\left(\mathbf{u}_j^n\right)+\frac{\rho_{\mathcal{O}}}{\rho_{\mathcal{A}}}V\left(\mathbf{v}_j^n\right)\right)=\lim_{n\to\infty}\left(V\left(\nabla\mathbf{u}_j^n\right)+\frac{\rho_{\mathcal{O}}}{\rho_{\mathcal{A}}}V\left(\nabla\mathbf{v}_j^n\right)\right)=0,$$

for all j.

Proof. Insert $\tilde{\mathbf{u}} = \mathbf{u}_j^{n+1}$ and $\tilde{q} = p_j^{n+1}$ in (55), apply the polarization identity, multiply through by Δt and take the ensemble average to see that

$$\begin{aligned}
&\frac{1}{4}\left\langle\left\|\mathbf{u}_j^{n+1}\right\|^2\right\rangle+\frac{1}{4}\left\langle\left\|2\mathbf{u}_j^{n+1}-\mathbf{u}_j^n\right\|^2\right\rangle-\frac{1}{4}\left\langle\left\|\mathbf{u}_j^n\right\|^2\right\rangle-\frac{1}{4}\left\langle\left\|2\mathbf{u}_j^n-\mathbf{u}_j^{n-1}\right\|^2\right\rangle\\
&+\frac{1}{4}\left\langle\left\|\mathbf{u}_j^{n+1}-2\mathbf{u}_j^n+\mathbf{u}_j^{n-1}\right\|^2\right\rangle\\
&+\Delta t\left\langle a_{\mathcal{A}}(\mathbf{u}_j^{n+1},\mathbf{u}_j^{n+1})\right\rangle+\Delta t\left\langle\widetilde{a_{\mathcal{A}}}(\mathbf{u}_j^{n+1},\mathbf{u}_j^{n+1})\right\rangle+\Delta t\,\gamma_{\mathcal{A}}\left\langle\left\|\nabla\cdot\mathbf{u}_j^{n+1}\right\|^2\right\rangle\\
&+\Delta t\int_{\Gamma_I}\left\langle\mathcal{I}_{\mathcal{A}}\left(\mathbf{u}_j^{n+1},\mathbf{v}_j^{n+1},\mathbf{u}_j^n,\mathbf{v}_j^n\right)\cdot\mathbf{u}_j^{n+1}\right\rangle d\Gamma_I=\Delta t\left\langle(\mathbf{f}_{\mathcal{A}}{}_j^{n+1},\mathbf{u}_j^{n+1})_{\mathcal{A}}\right\rangle.
\end{aligned}$$

On the other hand, take the ensemble average of (55) before inserting $\tilde{\mathbf{u}} = \mathbf{u}$. Then similar arguments may be used to show that

$$\begin{aligned}
&\frac{1}{4}\left\|\mathbf{u}^{n+1}\right\|^2+\frac{1}{4}\left\|2\mathbf{u}^{n+1}-\mathbf{u}^n\right\|^2-\frac{1}{4}\left\|\mathbf{u}^n\right\|^2-\frac{1}{4}\left\|2\mathbf{u}^n-\mathbf{u}^{n-1}\right\|^2\\
&+\frac{1}{4}\left\|\mathbf{u}^{n+1}-2\mathbf{u}^n+\mathbf{u}^{n-1}\right\|^2\\
&+\Delta t\,a_{\mathcal{A}}(\mathbf{u}^{n+1},\mathbf{u}^{n+1})+\Delta t\,\widetilde{a_{\mathcal{A}}}(\mathbf{u}^{n+1},\mathbf{u}^{n+1})+\Delta t\,\gamma_{\mathcal{A}}\left\|\nabla\cdot\mathbf{u}^{n+1}\right\|^2\\
&+\Delta t\int_{\Gamma_I}\left\langle\mathcal{I}_{\mathcal{A}}\left(\mathbf{u}_j^{n+1},\mathbf{v}_j^{n+1},\mathbf{u}_j^n,\mathbf{v}_j^n\right)\right\rangle\cdot\mathbf{u}^{n+1}\,d\Gamma_I=\Delta t\,(\mathbf{f}_{\mathcal{A}}{}^{n+1},\mathbf{u}^{n+1})_{\mathcal{A}}.
\end{aligned}$$

Now subtract this from the previous equation and apply Lemma 7 and (36) to see that

$$\begin{aligned}
&\frac{1}{4}V\left(\mathbf{u}_j^{n+1}\right)+\frac{1}{4}V\left(2\mathbf{u}_j^{n+1}-\mathbf{u}_j^n\right)-\frac{1}{4}V\left(\mathbf{u}_j^n\right)-\frac{1}{4}V\left(2\mathbf{u}_j^n-\mathbf{u}_j^{n-1}\right)\\
&+\frac{1}{4}V\left(\mathbf{u}_j^{n+1}-2\mathbf{u}_j^n+\mathbf{u}_j^{n-1}\right)+\Delta t\,\gamma_{\mathcal{A}}\left\langle\left\|\nabla\cdot(\mathbf{u}_j^{n+1})'\right\|^2\right\rangle\\
&+\Delta t\,(\nu_{\mathcal{A}}{}^H+\widetilde{\nu_{\mathcal{A}}}{}^H)V\left((\nabla\mathbf{u}_j^{n+1})^H\right)+\Delta t\,(\nu_{\mathcal{A}}{}^{\perp}+\widetilde{\nu_{\mathcal{A}}}{}^{\perp})V\left((\nabla\mathbf{u}_j^{n+1})^{\perp}\right)\\
&+\Delta t\int_{\Gamma_I}\left\langle\mathcal{I}_{\mathcal{A}}\left(\mathbf{u}_j^{n+1},\mathbf{v}_j^{n+1},\mathbf{u}_j^n,\mathbf{v}_j^n\right)\cdot\left(\mathbf{u}_j^{n+1}\right)'\right\rangle d\Gamma_I=0.
\end{aligned}\tag{58}$$

Note that the forcing terms cancel by assumption. The analogous steps may be applied with (56) and the result added to (58). For the viscous terms, bound below using Lemma 7 and Lemma 2. For a more compact notation, define

$$\begin{aligned}
\omega^{n+1}&\equiv V\left(\mathbf{u}_j^{n+1}\right)+\frac{\rho_{\mathcal{O}}}{\rho_{\mathcal{A}}}V\left(\mathbf{v}_j^{n+1}\right)\\
\beta^{n+1}&\equiv V\left(\nabla\mathbf{u}_j^{n+1}\right)+\frac{\rho_{\mathcal{O}}}{\rho_{\mathcal{A}}}V\left(\nabla\mathbf{v}_j^{n+1}\right)\\
\lambda^{n+1}&\equiv V\left(2\mathbf{u}_j^{n+1}-\mathbf{u}_j^n\right)+\frac{\rho_{\mathcal{O}}}{\rho_{\mathcal{A}}}V\left(2\mathbf{v}_j^{n+1}-\mathbf{v}_j^n\right)\\
\Lambda^{n+1}&\equiv V\left(\mathbf{u}_j^{n+1}-2\mathbf{u}_j^n+\mathbf{u}_j^{n-1}\right)+\frac{\rho_{\mathcal{O}}}{\rho_{\mathcal{A}}}V\left(\mathbf{v}_j^{n+1}-2\mathbf{v}_j^n+\mathbf{v}_j^{n-1}\right)\\
\Omega^{n+1}&\equiv\left\langle\gamma_{\mathcal{A}}\left\|\nabla\cdot(\mathbf{u}_j^{n+1})'\right\|^2\right\rangle+\frac{\rho_{\mathcal{O}}}{\rho_{\mathcal{A}}}\left\langle\gamma_{\mathcal{O}}\left\|\nabla\cdot(\mathbf{v}_j^{n+1})'\right\|^2\right\rangle.
\end{aligned}$$

In summary, it holds that

$$\begin{aligned}
&\frac{1}{4}\left(\omega^{n+1}+\lambda^{n+1}-\omega^{n}-\lambda^{n}\right)+\frac{1}{4}\Lambda^{n+1}+\frac{\Delta t}{2}\left\{2\Omega^{n+1}+\alpha_2\omega^{n+1}+\alpha_1\beta^{n+1}\right\}\\
&+\Delta t\int_{\Gamma_I}\left\langle\mathcal{I}_{\mathcal{A}}\left(\mathbf{u}_j^{n+1},\mathbf{v}_j^{n+1},\mathbf{u}_j^{n},\mathbf{v}_j^{n}\right)\cdot\mathbf{u}_j^{n+1}\right\rangle d\Gamma_I\\
&-\Delta t\int_{\Gamma_I}\left\langle\mathcal{I}_{\mathcal{A}}\left(\mathbf{u}_j^{n+1},\mathbf{v}_j^{n+1},\mathbf{u}_j^{n},\mathbf{v}_j^{n}\right)\right\rangle\cdot\mathbf{u}^{n+1}\,d\Gamma_I\\
&+\Delta t\int_{\Gamma_I}\left\langle\mathcal{I}_{\mathcal{O}}\left(\mathbf{u}_j^{n+1},\mathbf{v}_j^{n+1},\mathbf{u}_j^{n},\mathbf{v}_j^{n}\right)\cdot\mathbf{v}_j^{n+1}\right\rangle d\Gamma_I\\
&-\Delta t\int_{\Gamma_I}\left\langle\mathcal{I}_{\mathcal{O}}\left(\mathbf{u}_j^{n+1},\mathbf{v}_j^{n+1},\mathbf{u}_j^{n},\mathbf{v}_j^{n}\right)\right\rangle\cdot\mathbf{v}^{n+1}\,d\Gamma_I\le 0.
\end{aligned}$$

Next, apply Lemma 11 for the interface terms, sum over the time index and multiply through by 4. The result is

(59)

$$\begin{aligned}
&\omega^N+\lambda^N+4\Delta t\,R^N+2\Delta t\sum_{n=1}^{N-1}\left\{2S^{n+1}+2\Omega^{n+1}+\frac{1}{2}\Lambda^{n+1}+\alpha_2\omega^{n+1}+\alpha_1\beta^{n+1}\right\}\\
&\le\lambda^1+\omega^1+4\Delta t\,R^1.
\end{aligned}$$

In the limit as $N\to\infty$, it is necessary that

$$\lim_{n\to\infty}\omega^n=\lim_{n\to\infty}\beta^n=0.$$

This is the desired result. □

6. Computational testing

Here, heat transport is considered under conditions of (approximate) radiative equilibrium, as an example of an important process in AOI research [8]. Based on Theorem 2, it is likely that the conclusions of Theorem 3 still hold when ensembles are run with uncertainty in forcings, $\mathbf{f}_{\mathcal{A}j}$ and $\mathbf{f}_{\mathcal{O}j}$, and friction coefficients, κ_j. The statistical convergence of the CTM methods is investigated in this section.

The methods M, P1 and P2 will be tested in 2D domains $\Omega_{\mathcal{A}}=[0,10L]\times[0,L]$ and $\Omega_{\mathcal{O}}=[0,10L]\times[-L,0]$, where $L=500$ is a length scale in meters. The computational meshes in both domains are uniform Delaunay-Voronoi triangulations with mesh size $h=50\sqrt{2}$ (meters). Time steps are uniform, with size $\Delta t=5$ (seconds). These parameters are fixed throughout the computations below.

6.1. Heat convection model background state. A background flow state is computed in order to provide a uniform point of comparison for the CTM models. Whereas ensemble indices take on values $j=1,2,\ldots$, the background state will be associated with index $j=0$. Buoyancy-driven forcings for the momentum are used, which take the form

$$\mathbf{f}_{\mathcal{A}0}=\left\langle 0,-g(1-\beta_{\mathcal{A}}(\theta_0-\overline{\theta}_0))\right\rangle\quad\text{and}\quad\mathbf{f}_{\mathcal{O}0}=\left\langle 0,-g(1-\beta_{\mathcal{O}}(\psi_0-\overline{\psi}_0))\right\rangle.$$

Here, θ_0 and ψ_0 are temperatures in Kelvin (K), $g=9.81\,m\cdot s^{-2}$ is gravitational acceleration and $\beta_{\mathcal{A}}=3.43\cdot10^{-3}\,(K^{-1})$, $\beta_{\mathcal{O}}=2.07\cdot10^{-4}\,(K^{-1})$ are coefficients of thermal expansion for air and sea water. The temperature averages over domains $\Omega_{\mathcal{A}}$ and $\Omega_{\mathcal{O}}$ are denoted by $\overline{\theta}_0$ and $\overline{\psi}_0$, respectively.

The temperatures will be numerically approximated as solutions of the heat convection model

$$\begin{aligned} \partial_t \theta_0 - \alpha_{\mathcal{A}} \Delta \theta_0 + \mathbf{u}_0 \cdot \nabla \theta_0 &= 0 \text{ on } \Omega_{\mathcal{A}} \times (0,T], \\ \partial_t \psi_0 - \alpha_{\mathcal{O}} \Delta \psi_0 + \mathbf{v}_0 \cdot \nabla \psi_0 &= 0 \text{ on } \Omega_{\mathcal{O}} \times (0,T], \end{aligned}$$

with initial conditions discussed later. The (positive, constant) parameters $\alpha_{\mathcal{A}}$ and $\alpha_{\mathcal{O}}$ are thermal diffusivity parameters. These values are defined in terms of the Prandtl numbers (see [12]) for air ($Pr_{\mathcal{A}}$) and seawater ($Pr_{\mathcal{O}}$) by setting $\alpha_{\mathcal{A}} = {\nu_{\mathcal{A}}}^H / Pr_{\mathcal{A}}$ and $\alpha_{\mathcal{O}} = {\nu_{\mathcal{O}}}^H / Pr_{\mathcal{O}}$. The solutions are horizontally periodic, as described for the velocity and pressure variables. No heat flux is allowed through the bottom of $\Omega_{\mathcal{O}}$. Heat may be transferred across the fluid-fluid interface and through the model top (top of $\Omega_{\mathcal{A}}$), according to the boundary conditions

$$\begin{aligned} -c_{\mathcal{A}} \rho_{\mathcal{A}} \alpha_{\mathcal{A}} \nabla \theta_0 \cdot \hat{\mathbf{n}}_{\mathcal{A}} &= C^{ir}(\theta_0 - 285), \text{ on } \Gamma_t, \\ -c_{\mathcal{A}} \rho_{\mathcal{A}} \alpha_{\mathcal{A}} \nabla \theta_0 \cdot \hat{\mathbf{n}}_{\mathcal{A}} &= Q, \text{ on } \Gamma_I, \\ \text{and } c_{\mathcal{O}} \rho_{\mathcal{O}} \alpha_{\mathcal{O}} \nabla \psi_j \cdot \hat{\mathbf{n}}_{\mathcal{O}} &= Q, \text{ on } \Gamma_I, \end{aligned}$$

with heat flux Q on the interface consisting of three parts:

$$\begin{aligned} Q &= 30(1 - C^{alb})(1 + \cos((x - 150)\pi/150)) \text{ (solar radiative flux)} \\ &+ C^{ir}(\theta_0 - \psi_0) \text{ (longwave radiative flux)} \\ &+ C^{sen}|\mathbf{u}_0 - \mathbf{v}_0|(\theta_0 - \psi_0) \text{ (sensible heat flux).} \end{aligned}$$

The constants $c_{\mathcal{A}}$ and $c_{\mathcal{O}}$ are the specific heats of air and seawater, respectively. The condition on the model top drives the temperature toward the value $285\,K$ by allowing heating (or cooling) if θ_0 is below (or above) this value. The net heat flux Q can be either upward or downward, depending on the net solar radiative flux and the relative temperatures across the interface. The parameter C^{alb} is the albedo of the ocean. The solar heating is allowed to vary in space, otherwise even heating in these tests would inhibit circulation.

The numerical approximation for temperature uses globally-continuous, piecewise quadratic finite elements in space and BDF-2 in time, analogous to method M for the coupling terms, except that the velocities are also extrapolated there;

$$|\mathbf{u}_0 - \mathbf{v}_0|(\theta_0 - \psi_0)|_{t=t^{n+1}} \approx |E(\mathbf{u}_0^{n+1}) - E(\mathbf{v}_0^{n+1})|(\theta_0^{n+1} - \psi_0^{n+1}).$$

This decouples the temperature and velocity at each time step. A similar method was studied in [4] and shown to be numerically stable; the main difference is the BDF-2 time stepping, which can be analyzed as in [10]. The temperature fields are only computed as described here for the background state. Perturbed temperature fields are discussed later.

6.2. Model spin-up. A spin-up step was used to generate initial conditions for subsequent testing, with the goal of first bringing the background state near radiative equilibrium. This was achieved by starting with zero initial velocity and pressure, and uniform temperatures of $285\,K$ in $\Omega_{\mathcal{A}}$ and $300\,K$ in $\Omega_{\mathcal{O}}$. Method M was used to spin up the background state. Parameter values are shown in Table 3.

During spin-up, solar heating induces buoyancy-driven currents. The lower domain loses heat into the upper domain, due to the initial temperature differential. Since heat in the upper domain can radiate through the model top, the average temperatures in both domains stabilize. The problem was run for 20,000 time steps. Upon completion, the time-rate of change of average temperature in each subdomain was found to be below 10^{-7} in size. Although the system achieves an

TABLE 3. Physical parameter values in SI units for the background state.

$\nu_{\mathcal{A}}{}^{H}$	$\nu_{\mathcal{A}}{}^{\perp}$	$\nu_{\mathcal{O}}{}^{H}$	$\nu_{\mathcal{O}}{}^{\perp}$	$Pr_{\mathcal{A}}$	$Pr_{\mathcal{O}}$	$\gamma_{\mathcal{A}}$	$\gamma_{\mathcal{O}}$
1	20	1/15	20/15	0.713	7.2	1000	1000
$\rho_{\mathcal{A}}$	$\rho_{\mathcal{O}}$	$c_{\mathcal{A}}$	$c_{\mathcal{O}}$	κ_0	C^{ir}	C^{sen}	C^{alb}
1.2041	1025.0	1004.9	3993.0	0.5	6.0322	0.0011	0.1

approximate radiative equilibrium, the dynamics are not steady, as may be seen by looking at the total kinetic energies over time. These are given by

$$\frac{\rho_{\mathcal{A}}}{2}\int_{\Omega_{\mathcal{A}}} |\mathbf{u}|^2\, d\mathbf{x} \quad \text{and} \quad \frac{\rho_{\mathcal{O}}}{2}\int_{\Omega_{\mathcal{O}}} |\mathbf{v}|^2\, d\mathbf{x},$$

shown in Figure 1. The time step size is constrained by the faster dynamics in $\Omega_{\mathcal{A}}$.

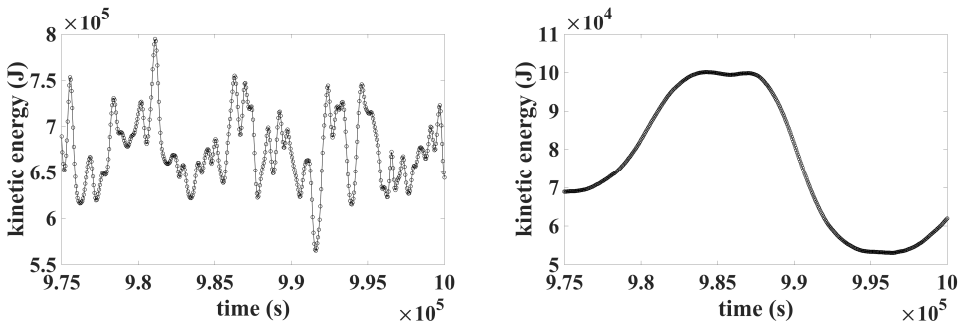

FIGURE 1. Kinetic energy during spin-up for the last 500 time steps in domains $\Omega_{\mathcal{A}}$ (left) and $\Omega_{\mathcal{O}}$ (right). The system is approximately at radiative equilibrium, but not stationary.

Temperature and velocity streamlines are shown in Figure 2. Although the system is quite simple compared to an atmosphere-ocean simulation, some similarities exist. Faster convective currents persist in $\Omega_{\mathcal{A}}$, compared to those in $\Omega_{\mathcal{O}}$. The kinetic energy in $\Omega_{\mathcal{O}}$ is still considerable, as a result of the larger density, $\rho_{\mathcal{O}} \approx \rho_{\mathcal{A}} \cdot 10^3$. A test could be done with a wider range of flow scales by decreasing the kinematic viscosities or by increasing the length scale, L. The parameter choices in this report are limited by the computational cost.

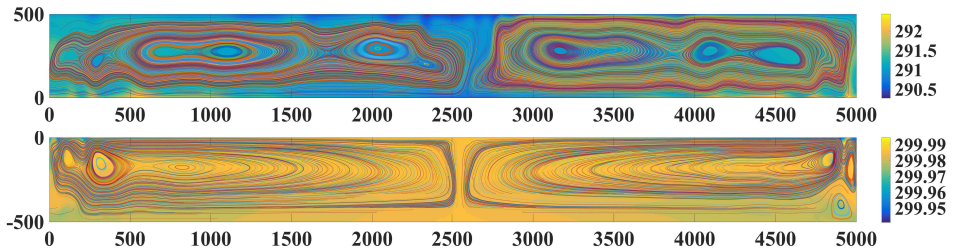

FIGURE 2. Streamlines and temperatures in $\Omega_{\mathcal{A}}$ (top) and $\Omega_{\mathcal{O}}$ (bottom) are shown for the initial conditions generated via spin-up. The flow exhibits a moderate range of flow scales.

6.3. Convergence to statistical equilibrium. The calculation of mean-flow kinetic energy (an example quantity of interest) and the convergence to statistical equilibrium are investigated with the CTM methods M, P1 and P2. Uncertainty is introduced through the Boussinesq forcing and the friction parameter. The initial conditions, shown in Figure 2, are not perturbed and do not contribute to the model variance. The constant parameters in Table 3 are used here. Ten-member ensembles are used, with uncertain data expressed in terms of the numbers

$$\delta_j = \begin{cases} -j, & j = 1, \dots, 5 \\ j - 5, & j = 6, \dots, 10 \end{cases}.$$

The friction parameters are $\kappa_j = \kappa_0 + 0.01\,\delta_j\,h(t)\,\kappa_0,\ j = 1, \dots, 10$. Note that $\sum_{j=1}^{10} \delta_j = 0$. The mean friction parameter is thus $\kappa = \kappa_0$.

The simulation is run for 2000 time steps, which yields a final time of $10^5\,s$. The function $h(t)$ is given by

$$0 \leq h(t) = \frac{t^2}{2.5 \cdot 10^7} \exp(2 - t/2500) \leq 1,$$

which satisfies $0 \leq h(t) \leq h(5000) = 1$ and decays to $h(10^5) \approx 10^{-14}$, so that (49) will hold.

Perturbed forcings are constructed to induce small-scale velocity fluctuations. The background temperature fields are perturbed to drive the flows, according to

$$\mathbf{f}_{\mathcal{A}j} = \left\langle 0, -g(1 - \beta_{\mathcal{A}}(\theta_0 - \overline{\theta}_0 + (5 \cdot 10^{-5})\delta_j\,h(t)^2 \cos(\pi\,x/250) \sin(\pi\,y/250)))\right\rangle$$
$$\mathbf{f}_{\mathcal{O}j} = \left\langle 0, -g(1 - \beta_{\mathcal{O}}(\psi_0 - \overline{\psi}_0 + (5 \cdot 10^{-6})\delta_j\,h(t)^2 \cos(\pi\,x/250) \sin(\pi\,y/250)))\right\rangle.$$

The full heat convection model is only used to calculate the background state ($j = 0$) at each time step. The ensemble only includes $j = 1, \dots, 10$, which are perturbations of the background state. The forcings for the ensemble members do not depend on the velocities $\mathbf{u}_j$ or $\mathbf{v}_j$, since this would present a fundamental deviation from the theory in this paper. The relative sizes of perturbations for κ_j, $\mathbf{f}_{\mathcal{A}j}$ and $\mathbf{f}_{\mathcal{O}j}$ reflect an attempt to balance out the contributions to model variance from these sources.

In addition to the CTM methods, a straight ensemble calculation is included here for comparison. That is, the numerical method equivalent to method M, but without using the mean-flow velocity for the convection terms and without any turbulent viscosity. Variance calculations in the L^2-norm are shown in Figure 3, and kinetic energy is shown in Figure 4. For the CTM methods, the turbulent viscosities were calculated using (22) with $\mu = 1.0$ in $\Omega_{\mathcal{A}}$, $\mu = 0.5$ in $\Omega_{\mathcal{O}}$, and l, k' defined in Table 2. These μ values were found to be roughly optimal for the mean-flow kinetic energy using method M to match the mean-flow kinetic energy without CTM as best as possible.

The model variance is consistent amongst CTM methods, but reduced compared to the variance without CTM, and vanishing in all cases. This is consistent with the implication of Theorem 2 and with Theorem 3. The kinetic energy is only shown on time intervals where variance is significant; details are hard to see on the global time scale. The CTM methods all track the reference mean-flow kinetic energy (without CTM) very well, in particular when the mean flow deviates significantly from the background state. When the variance is small, the mean-flow and background energies nearly coincide, but the partitioned methods predict a slightly different result in these regions, shown in Figure 5. Methods P1 and P2 predict the same energy when the variance in small, which is expected since these methods are equivalent when the variance is zero.

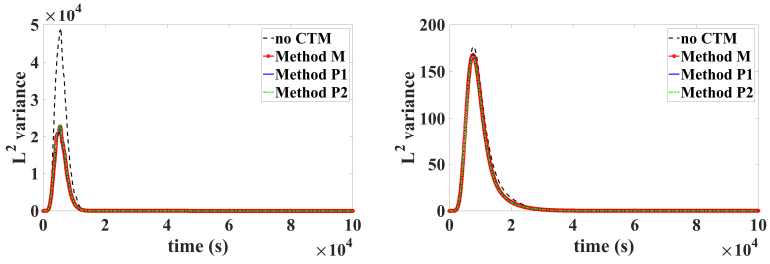

FIGURE 3. The variance (L^2-norm) in domains $\Omega_{\mathcal{A}}$ (left) and $\Omega_{\mathcal{O}}$ (right). As expected, the CTM methods have reduced the variance.

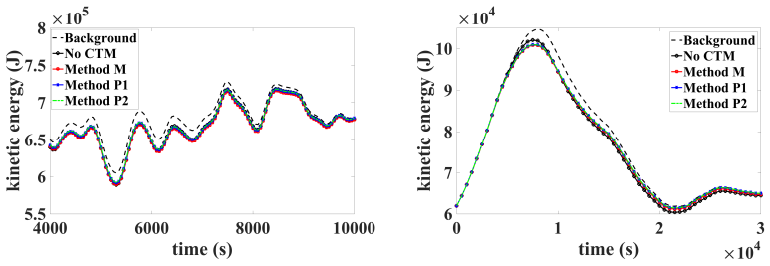

FIGURE 4. The background state and mean-flow kinetic energies in domains $\Omega_{\mathcal{A}}$ (left) and $\Omega_{\mathcal{O}}$ (right). The CTMs closely track the mean-flow behavior as it deviates from the background state.

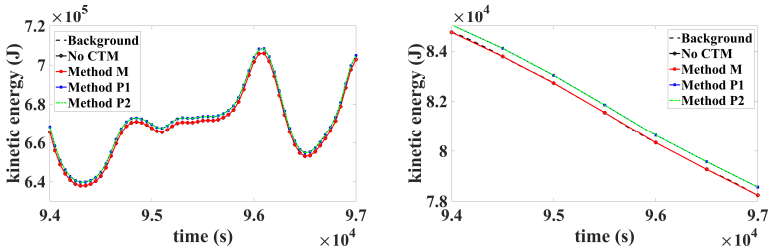

FIGURE 5. The background state and mean-flow kinetic energies in domains $\Omega_{\mathcal{A}}$ (left) and $\Omega_{\mathcal{O}}$ (right). The model variances are very small for the range of times shown here. The kinetic energy of the background state coincides with that of the mean-flow states without CTM and with method M, but methods P1 and P2 display a slightly different behavior.

Since the difference between the monolithic and partitioned methods is only the numerical coupling, the results suggest that the coupling method can introduce a statistical bias. In scientific AOI codes, this sort of bias would be challenging to quantify since (1) monolithic coupling is not available and (2) the coupling frequency is limited, due to the computational cost. Method P1 is more interesting than methods M or P2, for practical purposes. Aside from the issue of a statistical bias, the results shown here indicate that method P1 may (with parameter tuning) do a good job of reproducing mean-flow statistics.

7. Conclusions

A statistical turbulence model was proposed for ensemble calculations with two coupled fluids that enables some reduction in matrix assembly costs. The closure model accounts for the behavior of the Reynolds stress terms at the interface. The analyses of [10] were extended to account for the fluid coupling conditions, showing a proof of the Boussinesq hypothesis and squeezing of fluid trajectories with the turbulence model. Some numerical methods were proposed, including implicit and partitioned coupling, and it was proved for two methods that the discrete variance must vanish at long times. The analogous proof for the third partitioned method, which is of the most practical interest, is not known. But in computations this method was observed to predict almost exactly the same behavior as the other methods. Furthermore, the computations indicate an excellent ability for the turbulence methods to reproduce the correct ensemble mean-flow behavior. The partitioned methods may introduce a statistical bias at long times, which was small in the computational example.

Acknowledgments

The author thanks Professor William J. Layton for providing feedback regarding the development of this work.

References

[1] Alfonsi, G., Reynolds-averaged Navier-Stokes equations for turbulence modeling, Appl. Mech. Rev., Vol. 62 (2009), 1-20.
[2] Brezzi, F. and Falk, R. S., Stability of higher-order Hood-Taylor methods, SIAM Journal on Numerical Analysis, Vol. 28 (1991), No. 3, 581-590.
[3] Connors, J., Convergence analysis and computational testing of the finite element discretization of the Navier-Stokes-alpha model, Numerical Methods for Partial Differential Equations, Vol. 26 (2010), No. 6, 1328-1350.
[4] Connors, J. and Ganis, B., Stability of algorithms for a two-domain natural convection problem and observed model uncertainty, Computational Geosciences, Vol. 15 (2011), No. 3, 509-527.
[5] Connors, J., Howell, S. and Layton, W., Decoupled time stepping methods for fluid-fluid interaction, SIAM Journal on Numerical Analysis, Vol. 50 (2012), No. 3, 1297-1319.
[6] Galdi, G.P., An introduction to the mathematical theory of the Navier-Stokes equations: Steady-state problems, Springer Science and Business Media, 2011.
[7] Hood, P. and Taylor, C., A numerical solution of the Navier-Stokes equations using the finite element technique, Comp. and Fluids, Vol. 1 (1973), 73-100.
[8] IPCC, 2013: Climate Change 2013: The Physical Science Basis. Contribution of Working Group I to the Fifth Assessment Report of the Intergovern- mental Panel on Climate Change [Stocker, T.F., D. Qin, G.-K. Plattner, M. Tignor, S.K. Allen, J. Boschung, A. Nauels, Y. Xia, V. Bex and P.M. Midgley (eds.)]. Cambridge University Press, Cambridge, United Kingdom and New York, NY, USA, 1535 pp.
[9] Jiang, N. and Layton, W., Numerical analysis of two ensemble eddy viscosity numerical regularizations of fluid motion, Numerical Methods for Partial Differential Equations, Vol. 31 (2015), No. 3, 630-651.
[10] Jiang, N., Kaya, S. and Layton, W., Analysis of model variance for ensemble-based turbulence modeling, Computational Methods in Applied Mathematics, Vol. 15 (2015), No. 2, 173-188.
[11] John, V., Large Eddy Simulation of Turbulent Incompressible Flows, Springer-Verlag Berlin Heidelberg, 2004.
[12] Landau, L. D. and Lifshitz, E. M., Fluid Mechanics, Course of theoretic physics, Vol. 6, Pergamon Press, 1959, p. 203.
[13] Layton, W., Introduction to the numerical analysis of incompressible viscous flows, SIAM, 2008.
[14] Leray, J., Essay sur les mouvement d'un liquide visqueux que limitent des parois, J. Math. Pur. Appl. Paris Ser. IX, Vol. 13 (1934), 331-418.

[15] Leray, J., Sur le mouvement d'un liquide visqueux emplissant l'espace, Acta Mathematica, Vol. 63 (1934), No. 1, 193-248.
[16] Lions, J.-L., Temam, R. and Wang. S., Models for the coupled atmosphere and ocean (CAO I), Comput. Mech. Adv., Vol. 1 (1993), 1-54.
[17] Lions, J.-L., Temam, R. and Wang. S., Numerical analysis of the coupled atmosphere-ocean models (CAO II), Comput. Mech. Adv., Vol. 1 (1993), 55-119.
[18] Lions, J.-L., Temam, R. and Wang. S., Mathematical theory for the coupled atmosphere-ocean models (CAO III), J. Math. Pures. Appl., Vol. 74, (1995), 105-163.
[19] Manica, C. C., Neda, M., Olshanskii, M. and Rebholz, L.G., Enabling numerical accuracy of Navier-Stokes-α through deconvolution and enhanced stability, ESAIM: Mathematical Modelling and Numerical Analysis, Vol. 45 (2011), No. 2, 277-307.
[20] Mohammadi, B. and Pironneau, O., Analysis of the k-epsilon Turbulence Model, John Wiley and Sons, New York, 2009.
[21] Neale, R. B., *et. al.*, Description of the NCAR Community Atmosphere Model (CAM 5.0), NCAR Technical Note TN-486+STR, 2010.
[22] Rougier, J. S., David M. H., Murphy, J. M. and Stainforth, D., Analyzing the Climate Sensitivity of the HadSM3 Climate Model Using Ensembles from Different but Related Experiments, Journal of Climate, Vol. 22 (2009), No. 13, 3540-3557.
[23] Smith, *et. al.*, The Parallel Ocean Program (POP) Reference Manual, Los Alamos Technical Report LAUR-10-01853, 2010.

Department of Mathematics, University of Connecticut at Avery Point, Groton, CT, 06340, USA
E-mail: jeffrey.connors@uconn.edu
URL: http://www.math.uconn.edu/∼connors/